Alkali Activated Systems

Understanding the Influence of Curing Conditions and Activator Type/Chemistry on the Mechanical Strength and Chemical Structure of Fly Ash/Slag Systems

by

Ussala Chowdhury

A Thesis Presented in Partial Fulfillment
of the Requirements for the Degree
Master of Science

Approved July 2013 by the
Graduate Supervisory Committee:

Narayanan Neithalath, Chair
Barzin Mobasher
Subramaniam Rajan

ARIZONA STATE UNIVERSITY

August 2013

ABSTRACT

The alkali activation of aluminosilicate materials as binder systems derived from industrial byproducts have been extensively studied due to the advantages they offer in terms enhanced material properties, while increasing sustainability by the reuse of industrial waste and byproducts and reducing the adverse impacts of OPC production. Fly ash and ground granulated blast furnace slag are commonly used for their content of soluble silica and aluminate species that can undergo dissolution, polymerization with the alkali, condensation on particle surfaces and solidification. The following topics are the focus of this thesis: (i) the use of microwave assisted thermal processing, in addition to heat-curing as a means of alkali activation and (ii) the relative effects of alkali cations (K or Na) in the activator (powder activators) on the mechanical properties and chemical structure of these systems.

Unsuitable curing conditions instigate carbonation, which in turn lowers the pH of the system causing significant reductions in the rate of fly ash activation and mechanical strength development. This study explores the effects of sealing the samples during the curing process, which effectively traps the free water in the system, and allows for increased aluminosilicate activation. The use of microwave-curing in lieu of thermal-curing is also studied in order to reduce energy consumption and for its ability to provide fast volumetric heating.

Potassium-based powder activators dry blended into the slag binder system is shown to be effective in obtaining very high compressive strengths under moist curing conditions (greater than 70 MPa), whereas sodium-based powder activation is much weaker (around 25 MPa). Compressive strength decreases when fly ash is introduced into

the system. Isothermal calorimetry is used to evaluate the early hydration process, and to understand the reaction kinetics of the alkali powder activated systems. A qualitative evidence of the alkali-hydroxide concentration of the paste pore solution through the use of electrical conductivity measurements is also presented, with the results indicating the ion concentration of alkali is more prevalent in the pore solution of potassium-based systems. The use of advanced spectroscopic and thermal analysis techniques to distinguish the influence of studied parameters is also discussed.

ACKNOWLEDGMENTS

It would not have been possible to compile this master's thesis without the help and support of so many people in so many ways, to only some of whom it is possible to give mention here.

First and foremost, I would like to thank my husband Nabeel for his endless patience and encouragement at all times. My parents, sister, in-laws and extended family have always shown me their undeniable support throughout not only my academic career, but for anything and everything I've pursued, for which my mere expression of thanks does not suffice.

I would like to express my deep and sincere gratitude to my advisor, Dr. Narayanan Neithalath. I am extremely appreciative and indebted to him for the expert, sincere and valuable guidance he has extended to me throughout the learning process of this master's thesis. I also thank my thesis committee members, Dr. Subramaniam Rajan and Dr. Barzin Mobasher for consenting to assess my thesis.

I thank my lab mates Sundara and Akash for all their help and discourse during the course of this work. Special thanks go to Kirk for his time and helpful comments while preparing this document and for all his training and assistance as I familiarized myself with the laboratory equipment.

Finally, I would like to give acknowledgment to Arizona State University School of Sustainable Engineering and the Built Environment for funding me as both as a research and teaching assistant and permitting me to use their laboratory facilities which has allowed me to pursue my M.S. in Civil Engineering.

TABLE OF CONTENTS

Page

CHAPTER Page

CHAPTER Page

CHAPTER Page

LIST OF TABLES

Table Page

LIST OF FIGURES

Figure Page

Figure Page

Figure Page

Figure Page

Chapter 1

INTRODUCTION

The rapid growth in industrialization in the past decades has brought about the release of numerous undesirable pollutants into the atmosphere. The demand for portland cement based concrete has been ever increasing, despite the diminishing availability of natural resources. Moreover, the manufacturing process of portland cement raises issues of energy consumed (requiring temperatures up to 1400-1500°C), along with the detrimental effects of the greenhouse gases released to the environment. These issues have driven studies on the alkali activation of aluminosilicate materials as binder systems derived from industrial byproducts. They have been extensively studied due to the advantages they offer in terms enhanced material properties and sustainability resulting from the reuse of industrial waste and byproducts and reducing the adverse impacts of OPC production. The most commonly used source materials of these aluminosilicate binders are fly ash and ground granulated blast furnace slag, because of the presence of soluble silica and alumina species. When mixed with alkaline activators, these materials set and harden, delivering a material with very effective binding properties.

The source materials, activating alkali and the curing conditions are the most influential factors on the properties of the resulting product. The focus of this study touches on all these aspects, by exploring the influence of binder composition (fly ash, slag, or both), the effect of the alkali cation (K or Na) in powder activation, and the influence of curing conditions (moist curing, heat curing, microwave curing, in both sealed, and unsealed states).

Detailed experimental studies have been conducted to understand the early age properties and reaction kinetics of the binder. Reaction products formed in these systems have been characterized by means of advanced material characterization techniques, including Fourier Transform Infrared Spectroscopy (FTIR) and Thermogravimetric Analysis (TGA). It is expected that an increased understanding of the properties of these systems facilitated through this study will provide stimulus for the increased use of cement-free binder concretes.

1.1. Objectives

The main objectives of this study are listed below:

i. To evaluate the compressive strengths and microstructure of heat cured sodium silicate and sodium hydroxide activated fly ash concretes cured under various heat-treatment regimes (thermal curing and microwave curing) and exposure conditions during curing (sealed and unsealed);

ii. To understand the effects and fundamental differences of the alkali cation (K or Na) used on the powder activation of slag and fly ash-slag blends in terms of compressive strength, microstructure, and reaction product formation.

1.2. Thesis Layout

Chapter 2 provides a literature review of past studies on alkali activated binder systems. This includes a review on the reaction mechanisms of the alkali activated binders and their properties. It also provides a brief review on testing techniques used in the characterization of alkali activated binders.

Chapter 3 details the experimental design, including raw material properties, mixture proportions, mixing procedures and test methods used to assess the properties of the alkali activated fly ash and slag systems.

Chapter 4 discusses the findings of the studies with respect to the influence of heat-treatment techniques (conventional heat curing or microwave assisted thermal activation) and the exposure conditions on curing (sealed or unsealed) on the compressive strength and the reaction product formation and composition in alkali activated fly ash systems.

Chapter 5 is devoted to the understanding of the effect of the alkali cation used in the powder activation of slag and fly ash-slag blended binders. The difference in the reaction kinetics and mechanism when sodium and potassium silicates are used for the activation of these binders is brought out in this chapter.

Chapter 6 provides a detailed conclusion of the research studies carried out as part of this thesis.

Chapter 2

LITERATURE REVIEW

In this chapter the existing published work on the alkali activated fly ash, slag and other aluminosilicate materials as the binding medium is discussed.

2.1. Background and Overview

Industrialization leads to the production and expulsion of pollutants into the environment. With the increased emphasis on environmental protection, whilst maintaining the rapid pace of industrialization, it is necessary to investigate alternatives that do not cause detrimental effects to the environment. The reduction of greenhouse gas emissions and minimizing the energy consumed to create materials used for infrastructure are amongst the goals for environmental conservation. In the last 100 plus years, ordinary portland cement (OPC) has become amongst the most profusely used commodities worldwide. This extensive use comes at a high cost to the environment, as the production of OPC requires very high temperatures (1400-1500°C) and thus a large amount of energy and emission of greenhouse gases due to both chemical reactions during production and energy use. The production of one ton of OPC releases approximately one ton of CO_2 (Mahasenan, et al., 2003) and requires over 5000 MJ of energy (not including the energy required for quarrying raw materials) (Choate, 2003).

Another environmental concern is in regards to the consequences of improper waste disposal of industrial by-products, such as fly ash from coal burning for power generation and blast furnace slag from steel production. If unused, these industrial

byproducts are deposited in landfills. Landfilling is generally undesirable due to the high costs and the liability associated with the risk of contaminating ground water resources. In this context, industry has been looking for ways to recycle and reuse waste material as a better option to landfilling and disposing.

To overcome these problems, investigations on the alkali activation of aluminosilicate materials as binder systems derived from industrial byproducts have emerged. They have been extensively studied due to the advantages they offer in terms enhanced material properties, while contributing to sustainability through the reuse of industrial waste by-products and reducing the adverse impacts of OPC production. Fly ash and ground granulated blast furnace slag (GGBFS) are commonly used because of the high amounts of reactive silicate and aluminate species that can undergo dissolution, polymerization with the alkali, condensation on particle surfaces and solidification, providing the strength and stability to the binders. The resulting material was termed "geopolymers" by French scientist Joseph Davidovits in 1991.

Geopolymers can be used to bind loose aggregates together to form geopolymer concretes that can provide comparable performance to traditional cementitious binders in a range of applications with the added advantage of reducing greenhouse gas emissions and recycling industrial wastes (Duxson, et al., 2007). Depending on the starting raw material and processing conditions, alkali activated binders can exhibit a wide assortment of properties and characteristics, including high compressive strength, low shrinkage, fast or slow setting, resistance against chemical attack, fire resistance and low thermal conductivity (Duxson, et al., 2007).

2.2. Geopolymer Theory

Geopolymerization is a geosynthesis, a reaction that chemically integrates minerals (Khale & Chaudhary, 2007), in which aluminosilicate materials such as fly ash and slag are exposed to high-alkaline environments in the form of hydroxides or silicates. The alkali component in the activator is a compound from the first group in the periodic table, such that geopolymers are also termed "alkali activated alumino-silicate binders". These materials are characterized by a two- or three-dimensional Si-O-Al structure (McDonald & Thompson, n.d.), where silicon and aluminum atoms react to form molecules that are structurally and chemically similar to natural rocks (Hermann, et al., 1999). These binders have since been classified into three groups:

i. Binders manufactured with raw materials low in calcium and with high SiO_2 and Al_2O_3 contents. Fly ash is classified within this group. When activated with alkaline solutions, these materials modify into an amorphous material (alkaline aluminosilicate) that develops high mechanical strengths at early ages after gentle thermal curing.

ii. Binders synthesized from materials with composition rich in calcium such as GGBFS that produces calcium silicate hydrate (C-S-H) gel when activated with alkaline solutions (Alonso & Palomo, 2001).

iii. Binders manufactured from a blend of raw materials from the previous two groups, Ca, Si and Al rich material (Yip & Lukey, 2005; Palomo, et al., 2005).

The reaction mechanisms of these materials differ significantly from OPC. Portland cement relies on the presence of calcium to react with silica and form C-S-H gel for matrix and strength development; whereas geopolymers utilize the polycondensation of the silica and alumina precursors and a high alkali content to achieve structural strength (van Jaarsveld, et al., 2002).

2.2.1. Development of aluminosilicate binders

In order to examine the molecular structures of alkali activated binders or cement-free binders the term polysialate was coined as a descriptor of the silico-aluminate structure for this type of material. The network is configured of SiO_4 and AlO_4 tetrahedrons united by oxygen bridges (Figure 2-1), which has often been described to be similar to a sodalite network (Davidovits, 1999). Due to the negative charge of the Al tetrahedral in IV-fold coordination, positive ions must be present to balance out this charge. These ions (Na^+, K^+) must compensate the negative charge which is the reason why alkali silicates or hydroxides are used as the activating agents.

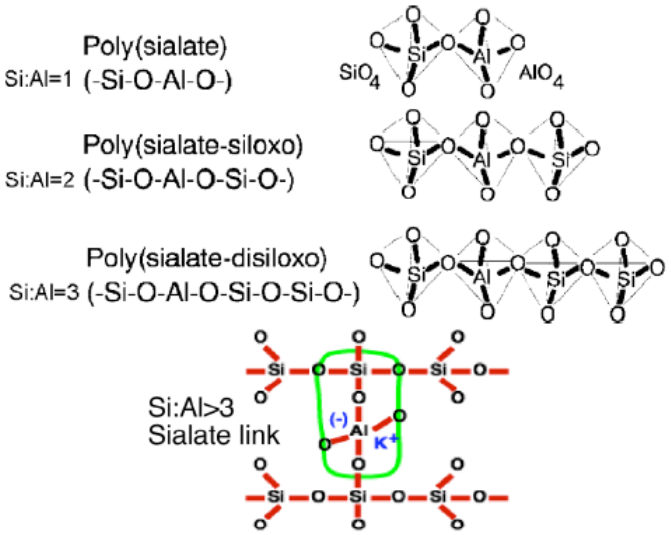

Figure 2-1: Aluminosilicate Structure and Nomenclature (Davidovits, 2005)

In the 1950s, a Ukrainian researcher named Glukhovsky (Glukhovsky, 1959) offered a general representation of the mechanism for the alkali-activation of compromising of silica and alumina species, which he termed as "soil-cements" in 1960s (Glukhovsky, 1965). Glukhovsky's model primarily divided the process into three distinct steps: (a) destruction-coagulation; (b) coagulation-condensation; (c) condensation-crystallization. Since then, different authors have elaborated on and extended Glukhovsky's theories with the added application of knowledge about zeolite synthesis. Davidovits took this forward expressing the reaction leading to the formation of a polysialate geopolymer as shown below: (Davidovits, 1999)

$$(Al_2Si_2O_7)_n + nH_2O \xrightarrow{MOH} n(OH)_3 - Si - Al - (OH)_3 \qquad \textbf{(2.3.2-1)}$$

$$n(OH)_3 - Si - O - Al - (OH)_3 \xrightarrow{MOH} M\left(-\underset{\underset{O}{|}}{\overset{|}{Si}} - O - \underset{\underset{O}{|}}{\overset{|}{Al^{(-)}}} - O\right)_n + n \qquad \textbf{(2.3.2-2)}$$

In the above equations, *M* is the cation used in the activation reaction which is generally introduced as either KOH or NaOH. Additional amounts of amorphous silica must be present in order to form either the polysialate-siloxo or polysialate-disiloxo structures of geopolymers. The reaction for the polysialate-siloxo formation is also provided below as an illustration of how the two reactions differ (Davidovits, 2005).

$$(Al_2Si_2O_7)_n + nSiO_2 + nH_2O \xrightarrow{MOH} \underset{\underset{(OH)_2}{|}}{n(OH)_3 - Si - O - Al - O - Si - (OH)_3} \qquad \textbf{(2.3.2-3)}$$

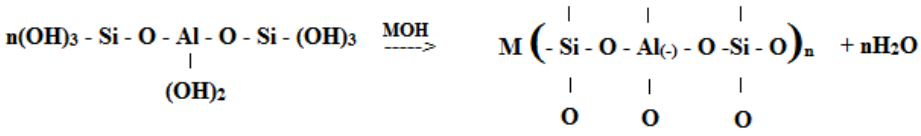

(2.3.2-4)

After the geopolymerization process is completed, the final geopolymer obtained is described by the empirical formula:

$$M_n\{-(SiO_2)z-(AlO_2)\}n + H_2O \qquad (2.3.2\text{-}5)$$

Here *M* again is a cation used to activate the reaction, *n* is the degree of polycondensation, and *z* = 1, 2, 3 for polysialate, polysialate-siloxo, and polysialate-disiloxo structures respectively. Figure 2-2 below illustrates a simplified model of the polymerization process of alkali-activated geopolymers as they transform from a solid aluminosilicate source into a synthetic alkali aluminosilicate.

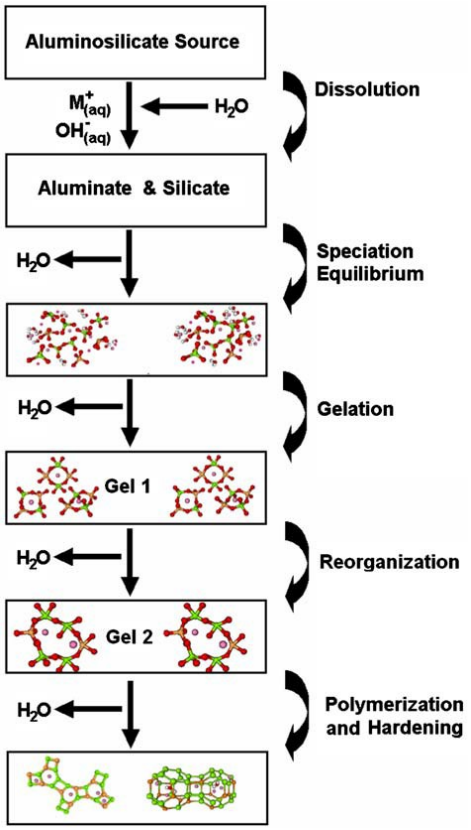

Figure 2-2: Conceptual model for geopolymerization process (Duxson, et al 2007)

Dissolution of the solid aluminosilicate source by the alkaline hydrolysis produces aluminate and silicate species (Duxson, et al., 2007). It occurs immediately upon contact between the alkaline activating solution and aluminosilicate source material, allowing for an ionic interface between species and breaking the covalent bonds to liberate the silicon, aluminum and oxygen atoms (Petermann, et al., 2010). Similar to OPC reactions, this step usually generates rapid and intense heat (as shown in isothermal calorimetric data in Chapter 5), and is directly proportional to the pH level and concentration of the activating solutions. The rate of dissolution is also a function of the amount and composition of the source material and pH of the activating solution (Fernández-Jiménez, et al., 2006).

Once dissolution is complete, the species released are incorporated into the aqueous phase, which may already contain free silicate from the activating solutions, providing a complete mixture of silicate, aluminate and aluminosilicate species. When activating solutions with a high pH are used, the dissolution is rapid and creates a supersaturated aluminosilicate solution. When the concentration reaches a substantial level, a gel starts to form as the oligomers in the aqueous phase form large networks consisting of Si-O-Al-O bonds through condensation. At this stage, water that was consumed during dissolution is released and plays the role of a reaction facilitator, residing within the pores of the gel. The formed gel is initially aluminum-rich and contains alkaline cations that compensate for the deficit charges produced with the aluminum-for-silicon substitution (Petermann, et al., 2010).

After gelation, the system continues to rearrange and reorganize as the connectivity of the gel network increases, resulting in a three-dimensional aluminosilicate

network, as represented in Figure 2-2 with the presence of multiple “gel stages”. (Duxson, et al., 2007)

2.2.2. Alkaline activation of fly ash

Fly ash is one of the residues generated in combustion of anthracite and bituminous coal. It is considered to be one of the most important sources of materials for alkali activated binders or for partial cement substitution in OPC blends. Unused fly ash in the past was generally released into the atmosphere, but recent pollution control laws require that it now be captured prior to release and generally has been stored at coal burning power plants or placed in landfills.

Fly ash is generally an acidic material containing acidic oxides such as Al_2O_3, SiO_2 and Fe_2O_3 which provide a potential for alkali reaction (Petermann, et al., 2010). Fly ash is usually grouped under two classifications: low-Ca fly ash or Class F fly ash and high-Ca fly or Class C fly ash. Class F is the more abundant of the two and is the preferred class for the synthesis of alkali activated concretes due to the high availability of reactive silica and alumina.

The alkali activation of fly ash occurs through an exothermic reaction with dissolution causing the covalent bonds in the glassy phase (Si-O-Si and Al-O-Al) to pass through the solution. These free species accumulate over a certain period of time (termed the “induction period”), during which heat release is generally low. After enough reactive ions have accumulated, the paste enters another highly exothermic stage where a condensation of the structure is produced resulting in a cementitious material with a poorly ordered structure, but high mechanical strength. This product is an amorphous

alkali aluminosilicate gel that has a structure similar to that of zeolitic precursors. The mechanism of geopolymerization describes this formation of reaction product as a layer around the fly ash particles and is shown in Figure 2-3 below. Figure 2-3a shows the dissolution process initiated by a chemical attack at one point on the surface of the particle, which then expands further (Figure 2-3b), exposing the smaller particles, whether hollow or partially filled with other yet smaller ash particles from the outside in and from the inside out. Consequently, reaction product is generated both inside and outside the shell of the sphere, until the ash particle is completely or almost completely consumed. At the same time, as the alkaline solution penetrates and contacts the smaller particles within the larger spheres, the interior space of the sphere starts to fill up with reaction product, forming a dense matrix.

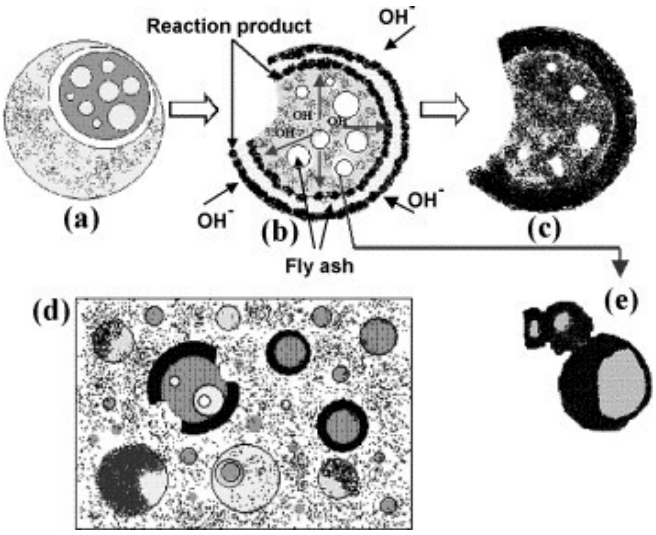

Figure 2-3: Descriptive model of the alkali activation of fly ash (Fernández-Jiménez, et al., 2005)

Most research into the topic of alkali activation of fly ash reveals that the reaction requires applied energy in the form of heat to attain reasonable mechanical properties.

2.2.3. Alkaline activation of ground granulated blast furnace slag (GGBFS)

Ground granulated blast furnace slag (GGBFS) is an industrial by-product of the smelting ore process, which is used to separate the desired metal fraction from the unwanted fraction. It is usually comprised of metal oxides and silicon dioxide, but can also contain metal sulfides and pure metal atoms in their elemental form. The alkali-activation of blast furnace slag has been used as an alternative to cement in concrete production for over 65 years (Roy, 1999; Purdon, 1940). Slag also contains calcium, resulting in a reaction that differs from that explained above. Alkalis initially attack the outer layer of the slag particles, breaking them up until ultimately a polycondensation of reaction products occurs. An initial stage of reaction products form during dissolution and precipitation, but at later stages a solid state mechanism takes place on the surface of the formed particles which is dominated by slow diffusion of the ionic species into the virgin core (Chithiraputhiran, 2012). In this reaction, the alkali cations (M^+) acts as a catalyst for the reaction in the initial stages of hydration as shown in the following equations, where the cations are exchanged with free Ca^{2+} ions: (Glukhovsky, 1994; Krivenko, 1994)

$$\mathbf{=Si\text{-}O\text{-} + M^+ \rightarrow =Si\text{-}O\text{-}M} \qquad \mathbf{(2.3.2\text{-}1)}$$

$$\mathbf{=Si\text{-}O\text{-}M + OH\text{-} \rightarrow =Si\text{-}O\text{-}M\text{-}OH^-} \qquad \mathbf{(2.3.2\text{-}2)}$$

$$\mathbf{=Si\text{-}O\text{-}M\text{-}OH\text{-} + Ca^{2+} \rightarrow =Si\text{-}O\text{-}Ca\text{-}OH + M^+} \qquad \mathbf{(2.3.2\text{-}3)}$$

As is evident, the alkaline cations perform the role of structure-templating. The nature of the anions also plays a role in activation reactions, particularly at early ages in regards to paste setting (Fernández-Jiménez & Puertas, 2001; Fernández-Jiménez, et al., 2003).

The final reaction products obtained are similar to those of OPC hydration (C-S-H gel, albeit with a lower Ca/Si ratio than those of OPC pastes), with the distinction being the rate and intensity of the reaction. Since slag contains reactive silica, it also exhibits pozzolanic activity in the presence of calcium hydroxide. Thus, when blended with OPC, there will be three distinct steps: cement hydration, slag hydraulic reaction and slag pozzolanic activity (Ravikumar, 2012).

2.2.4. Alkaline activation of blended binders

As mentioned in previous sections, the heat curing of fly ash as a sole binder requires thermal processing for activation. Since the energy implications of moist curing are much more favorable than those of heat curing, and disposal of fly ash is more challenging than that of slag, efforts have been made to develop alkali activated mixtures that consist of a larger proportion of fly ash, which can be moist cured to obtain acceptable mechanical properties (Chithiraputhiran & Neithalath, 2013; Chithiraputhiran, 2012). Both fly ash and slag are two common types of solid wastes with certain similarities in that they are both calcium alumino-silicates (with different ratios of constituents). However, there are also many distinguishing features. The amount of crystalline particles is much higher in fly ash systems consisting predominantly of spherical particles, whereas slag typically contains broken and fragmented particles. Fly ash is relatively rich in Al_2O_3 while slag is rich in CaO (Zhao, et al., 2007). In combining both materials the shortcomings of one can potentially be overridden by the merits of the other. The blending of these two source materials result in the creation of two reaction products. The main reaction product formed is a calcium silicate hydrate rich in Al,

which includes the alkali cation used in activation (Na or K) in its structure. The other reaction product which was formed in the pastes is a result of fly ash activation; an alkaline aluminosilicate hydrate with a three-dimensional structure (Puertas & Fernández-Jiménez, 2003).

With the exception of drying shrinkage, enhanced properties, such as compressive strength, flexural strength and water absorption, have been obtained in alkali activated fly ash-slag blended mortars than comparable OPC mortars (Chi & Huang, 2013). Where sodium based activators have been used, the early age strength gain has been decent, however there was little gain in later ages. Strength improvements may be obtained by varying fly ash-slag ratios or by increasing the fineness of the slag (Smith & Osborne, 1977). It has been found that the compressive strength increases with slag content. The inclusion of a little amount of lime showed vast improvements of the early age strength; however this caused a slight decrease in the later age strength of the activated fly ash-slag blends (Shi & Day, 1999). When NaOH is used as an activator, the fly ash type (Class C or Class F) used did not have a significant effect on the strength development, although where Class C fly ash was used, the hydration process was affected due to the presence of calcium. Studies have also found that when the proper dosage of fly ash is blended in to the system, the strength and pore structure properties all exceed that of the slag cement system. This is due to the pozzolanic filling effect of the fly ash (Li, et al., 2000).

Most previous studies employ sodium-based solutions in the activation of fly ash-slag blends. The present study compares the influence of both potassium and sodium silicates in powder form blended in directly to the binder system.

2.3. Alkaline activators and their properties

The activation of the selected binder materials contributes most significantly to producing a structurally sound material via the geopolymeric reaction process. It is the activator that prompts the dissolution, precipitation and crystallization of the aluminosilicate species. When hydroxides are used, the OH^- ions act as a catalyst for the reaction by aiding with the dissolution of the silica and alumina species of the source material and the metal cation (Na^+ or K^+) serves as a charge balancer for the aluminum framework when a Si^{4+} is substituted by an Al^{3+}. The initial steps of the alkali activation reaction process is thus dependent on the alkaline solutions' ability to dissolve the source binder material and release reactive silicon and aluminum into solution (Petermann, et al., 2010).

The alkaline solutions are derived using soluble alkali metals that are usually sodium or potassium based. The most common alkaline liquid used in geopolymerization is a combination of sodium hydroxide (NaOH) or potassium hydroxide (KOH) and sodium silicate ($Na_2O{\cdot}nSiO_2$) or potassium silicate ($K_2O{\cdot}nSiO_2$) (Rangan, 2008).

2.3.1. Alkali hydroxides as activating agents

The most commonly used activators are hydroxides of sodium (NaOH) and potassium (KOH). Since K^+ is more basic it provides a higher degree dissolution and polymeric ionization of the source material, leading to denser polycondensation reaction and more enhanced matrix formation. However, higher concentrations of KOH have been shown to decrease the resulting compressive strength due to excessive K^+ ions in the solution and leaching of the ions from the paste (Khale & Chaudhary, 2007).

While KOH is generally found to facilitate greater degrees of dissolution, NaOH actually has a greater ability to liberate silicate and aluminate monomers. This is due to sodium cations being much smaller than potassium cations and can migrate throughout the paste network, thus promoting better zeolitization (Rangan, 2008).

2.3.2. Alkali silicates as activating agents

Sodium (or potassium) silicates are manufactured by fusing sand (SiO_2) with sodium or potassium carbonates (Na_2CO_3 or K_2CO_3) at temperatures ranging from 1100-1200°C and subsequently dissolved with high pressure steam into a clear, semi-viscous fluid (McDonald & Thompson, n.d.). However, these alkali silicates are rarely ever used as an independent activating solution since they do not contain the required activation potential to initiate the geopolymeric process on its own. Instead, it is often mixed with an alkali hydroxide solution to enhance its alkalinity to ensure increased dissolution and product formation.

The ratio of silicate to hydroxide plays an important role in the compressive strength development of activated systems. In general, an increase in the concentration of the alkali (or decreasing the added soluble silicate) results in an increase of the compressive strength. This is because an excess of soluble silicates retards setting (through the delayed release of water and the polycondensation) and structure formation (Khale & Chaudhary, 2007). Thus, care must be taken to regulate the molar ratio of hydroxides to silicates.

2.4. Synthesis of Alkali Activated Binders

The production of a cement-free binder requires source material rich in aluminum and silicate species as the binder and alkali solutions for activation. Certain types of source material also necessitate the application of heat curing to obtain reasonable mechanical properties.

2.4.1. Common mixing procedures

The principal difference between geopolymer concretes and OPC concretes is in the binder paste. A geopolymer requires the addition of an alkali activator to react with the silicon and aluminum oxides in order for the strength imparting chemical processes to occur, thus binding the aggregates together to form the geopolymer concrete.

Studies have also found that when the source material contains calcium (such as slag or Class C fly ash), the setting time of the mixture is low and handling of the mixture is difficult due to early stiffening (Astutiningsih & Liu, 2005). This phenomena is more prevalent for systems activated with Na^+ cations than K^+ cations, since potassium has a better ability to dissolute and are also slightly less exothermic (as will be evident in later chapters).

2.4.2. Curing conditions

Activation of aluminosilicate binder that does not contain a calcium component generally requires heat curing to produce binders with suitable mechanical properties. A wide range of temperatures varying from 40°C to 90°C have been used in the past to produce alkali activated binders with adequate mechanical performance, with the general

trend showing that higher compressive strengths can be obtained when cured at higher temperatures (Ravikumar, et al., 2010; Ma, et al., 2012; Rangan, 2008). Alkali activated slag cements only require moist curing due to their potential to form calcium silicate hydrates as the reaction product as discussed previously.

For binders where heat curing is required, studies have also found that the application of heat-curing can be delayed for several days and not cause degradation of the final product. In some cases, such delays substantially increased the resulting compressive strength of the alkali activated concrete (Hardjito & Rangan, 2005). An increase in curing temperature has a positive effect on the compressive strength of the final binder created at early ages; however has the opposite effect at later ages, where lower curing temperatures exhibit higher compressive strengths.

A study on the effect of the heat curing conditions (sealed vs. unsealed) on the compressive strength and reaction product formation are explored in detail in Chapter 4.

2.4.3. Effects of microwave radiation on curing process

For the alkali activation of aluminosilicate binders that require a supply of activation energy in the form of heat to instigate the reaction, the most common process is through the use of thermal curing. However, thermal curing causes thermal gradients to occur throughout the specimen, as heat is applied to the surface and allowed to diffuse to the core via convection. This does not allow for uniform heating of the sample, which may result in undesirable properties. An alternative to heat curing is the use of microwave curing, where microwave energy is delivered directly to the material through interactions at the molecular level with the electromagnetic field (Somaratna, et al.,

2010). Microwave material interactions result in translational motions of the free and bound charges and the rotation of dipoles. The frictional, elastic and inertial forces that resist these motions instigates volumetric heating of the material. Thus, since the effect of the microwave energy is dependent on energy conversion rather than heat transfer, rapid and uniform heating is possible.

The dielectric constant (ε') and the dielectric loss factor (ε'') are used to describe the electromagnetic interactions at the atomic level that results in microwave heating. The dielectric constant is a measure of the material's ability to be polarized in response to the electric field. The dielectric loss factor measures the material's efficiency at converting the electric field into heat energy (Gubb, et al., 2011). Using these two factors, the dielectric permittivity (ε) of the material is given as:

$$\varepsilon = \varepsilon' - i\varepsilon'' \qquad \textbf{(2.4.3-1)}$$

The loss tangent ($\tan\delta$) represents the ratio of the dielectric loss factor to the dielectric constant. This parameter depends on the frequency of the microwave of the microwave radiation and the temperature (Somaratna, et al., 2010). A loss tangent between 0.01 and 1 generally indicates that the material will heat well with microwave energy. Any value below tends to be microwave transparent, while any value above is reflective (Shulman, et al., 2007). The rate of energy absorption is expressed as the power per unit volume (P) and is given as:

$$P = \omega\varepsilon_0\varepsilon''|E_{int}|^2 = \omega\varepsilon_0\varepsilon' tan\,\delta\,|E_{int}|^2 \qquad \textbf{(2.4.3-2)}$$

where ω is the angular frequency, ε_0 is the permittivity of free space (8.854×10^{-12} F/m), and E_{int} is the intensity of the internal electric field (Clark, et al., 2000). As is evident from the above equation, the dielectric properties exert a considerable influence on the absorbed power of the material. A significant portion of the absorbed power is then converted to heat within the material as:

$$\frac{\Delta T}{\Delta t} = \frac{P}{\rho C_p} = \frac{\omega \varepsilon_0 \varepsilon'' |E_{int}|^2}{\rho C_p} \quad \textbf{(2.4.3-3)}$$

where T is the temperature, t is the time, ρ is the density and C_p is the heat capacity (Clark, et al., 2000). Dielectric parameters influence the depth to which microwaves penetrate into the material, given by the equation:

$$D_p = \frac{1}{\frac{\omega}{v}\sqrt{\frac{\varepsilon''\left(\sqrt{1+(tan\,\delta)^2}-1\right)}{2}}} \quad \textbf{(2.4.3-4)}$$

where v is the microwave speed (Cha-um, et al., 2009). Taking approximate values of the dielectric parameters ε' and ε'' for concrete as 5.69 and 0.62 respectively (Büyüköztürk, et al., 2006), the penetration depth obtained is 5.9 in, which is larger than the specimen size. This confirms that volumetric heating does occur during the microwave curing process (Somaratna, et al., 2010).

Studies have also found that the SiO_4 and AlO_4^- tetrahedra networks are most likely transparent to microwaves, thus the energy absorbed by the material is primarily due to the dielectric heating of the pore solution (Gubb, et al., 2011).

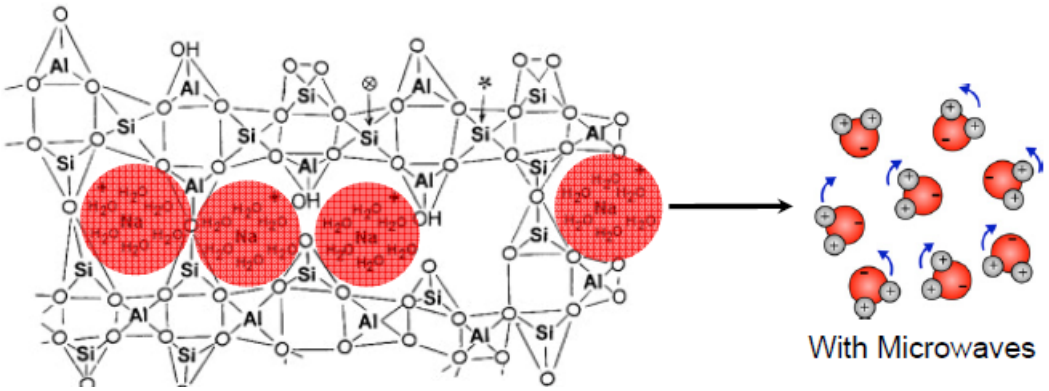

Figure 2-4: The dielectric heating of the concrete pore solution under microwave radiation (Gubb, et al., 2011)

2.5. Isothermal Calorimetric Studies to Evaluate Reaction Kinetics

The hydration of ordinary portland cement binders is in general a five step process of dissolution, induction, acceleration, deceleration and finally diffusion limited. This evolution can be qualitatively characterized by the heat evolution curve shown in Figure 2-5. The major activity during each stage is described as follows:

1. Pre-induction (Dissolution) – This is the initial rapid hydration that occurs when the particles of cement are exposed to water, releasing a large amount of heat. Duration: On the order of minutes.
2. Induction (Dormant) – A period of reduced hydration activity that allows for the transportation and placement of the mix. Duration: On the order of 1-2 h.
3. Acceleration – The rate of hydration increases. This is the beginning of the period during which the cement paste will achieve initial set. The major portion of the silicates hydrates and the cement solidifies. Duration: On the order of several hours.

4. Deceleration – The hydration rate decreases as the hydrated material covers the particles. Duration: On the order of hours to days.
5. Diffusion Controlled – Hydration and aggregation occur at a very low rate. Reactions are limited by the rate of diffusion of species through the dense pore network. Duration: On the order of days to years. (Bentz, et al., 1994)

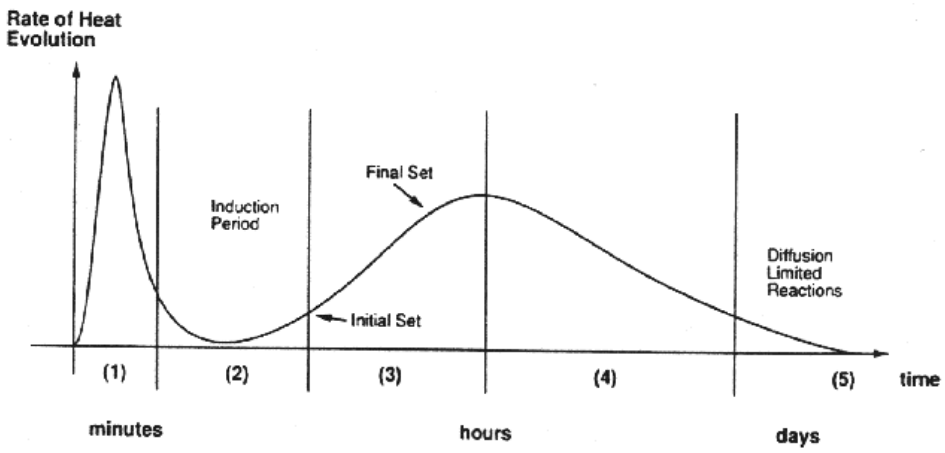

Figure 2-5: Heat evolution curve of cement hydration (Nelson, 1990)

In alkali activated systems with a calcium source, the primary reaction product is C-S-H with a low Ca/Si ratio. Its reaction kinetics are governed by the activator type, temperature and the alkalinity of the activator. In potassium silicate powder activated systems, the heat evolution response is similar to that of OPC hydration, as shown in Figure 2-5. The development of the peaks seems to have a direct relationship with the alkali concentration, with the time of occurrence decreasing with a decrease in alkali concentration.

It has been established that the initial pH of the activator plays a vital role in the initial dissolution of the binder and promoting the initial formation of hydration products. There are three models offered to describe the hydration of alkali activated slag cements. The first model describes the case where there is only one initial peak and no further peaks. The second model comprises of one peak before and after the dormant period, and finally the third model includes two peaks before the dormant period and one peak after (Shi & Day, 1995). The potassium silicate powder activated systems follow the trends of the second model, which is the most akin to ordinary portland cement systems. For sodium silicate powder activated binders, the reaction takes place so quickly that the dissolution and acceleration periods are combined with no induction period recorded (similar to the first model). There has not been much research on the case of these powder activated systems, which will be the focus of the research in Chapter 5.

2.6. Reaction product and microstructure analysis

2.6.1. Fourier transform Infra-Red (FTIR) spectroscopy analysis

Fourier Transform Infra-Red (FTIR) spectroscopy is a quick method for analyzing the reaction products formed in alkali activated binder systems. In infrared spectroscopy, infrared radiation is passed through a sample, where a portion of the radiation is absorbed and a portion is transmitted. The resulting spectrum represents the molecular absorption and transmission, creating a molecular fingerprint of the sample. This makes infrared spectroscopy useful for identification (qualitative generally, but quantitative also possible) of reaction products in these systems. Table 2-1 shows the common FTIR spectra peaks identified from literature for OPC and alkali activated pastes.

Table 2-1: Attributing FTIR peak signals to typical bonds (Yu et al. 1999)

Peak location (cm^{-1})	**Chemical bond characteristic of the signal**
3650	Hydrated Minerals (i.e. $Ca(OH)_2$)
3600-3100	S-O (Gypsum)
3400	OH Stretching (H_2O)
2930, 2850	Calcite Harmonic
1650	S-O (Gypsum) H-O-H Bending (H_2O)
1430	C-O Asymmetric Stretching
1100	S-O (Gypsum) Si-O-Si and Al-O-Si Asymmetric Stretching
1035-1030	aluminosilicate bonding
1010-1000	Calcium Silicates
960-800	Si-O, Al-O Stretching
872	C-O Bending
480	Si-O-Si and O-Si-O Bending

Chapter 3

MATERIALS, MIXTURE PROPORTIONS AND TEST METHODS

The purpose of this chapter is to describe the materials used and the methodology employed for the research presented in this thesis. The experimental procedures used to create the samples are also explained in detail, along with a description of the equipment utilized for the analysis.

3.1. Materials

The binder materials used in this study are Class F fly ash conforming to ASTM C 618 and ground granulated blast furnace slag (GGBFS) Type 100 conforming to ASTM C 989, the chemical compositions of which are shown in Table 3-1. The reactivity of these materials when activated with alkalis is predominantly dependent on the CaO, SiO_2 and Al_2O_3 contents of the binders. Figure 3-1 presents the CaO-SiO_2-Al_2O_3 ternary diagram indicating the location of the source materials by composition.

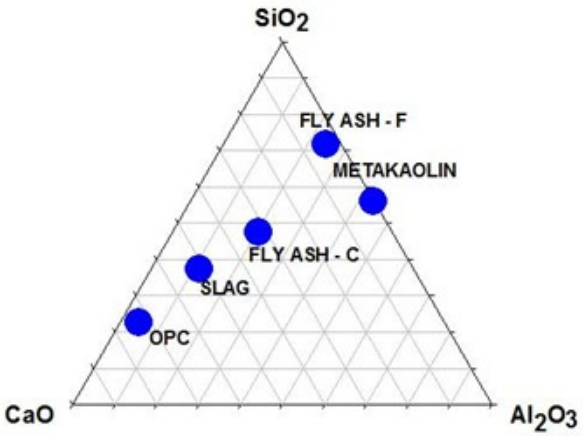

Figure 3-1: Ternary diagram illustrating the CaO-SiO_2-Al_2O_3 composition of different materials used in concrete production (Chithiraputhiran, 2012)

Table 3-1: Chemical composition and physical characteristics of Class F fly ash and slag

Chemical Analysis	**Class F Fly ash (Chapter 4)**	**Class F Fly ash (Chapter 5)**	**Slag**
Silicon Dioxide (SiO_2)	57.96%	59.62%	39.44%
Aluminum Oxide (Al_2O_3)	23.33%	23.03%	6.88%
Iron Oxide (Fe_2O_3)	4.61%	4.62%	0.43%
Calcium Oxide (CaO)	5.03%	4.87%	37.96%
Sulfur Trioxide (SO_3)	0.39%	0.48%	2.09%
Loss on Ignition (L.O.I)	0.45%	0.37%	3.00%
Sodium Oxide (Na_2O)	1.28%	2.32%	1.67%
Others	6.95%	4.69	8.53%
Density (g/cc)	2.28	2.25	2.9

All three of these binding materials are silica and alumina rich, which are necessary for the formation of the strength imparting phases in alkali activated binders. The silica-to-alumina ratios were found to be approximately 2.48, 2.59 and 5.73 for the fly ashes and slag used. In addition to the high silica and alumina content in slag, it also contains a high CaO content (~38%), while the CaO content in Class F fly ash is very low (5.03% and 4.87%) as expected.

The particle size distributions of the fly ash and slag (obtained using a laser particle size analyzer) are shown in Figure 3-2. The particle size analysis indicates that slag is finer than fly ash with 95% of particles finer than 30 μm compared to only 60% for fly ash.

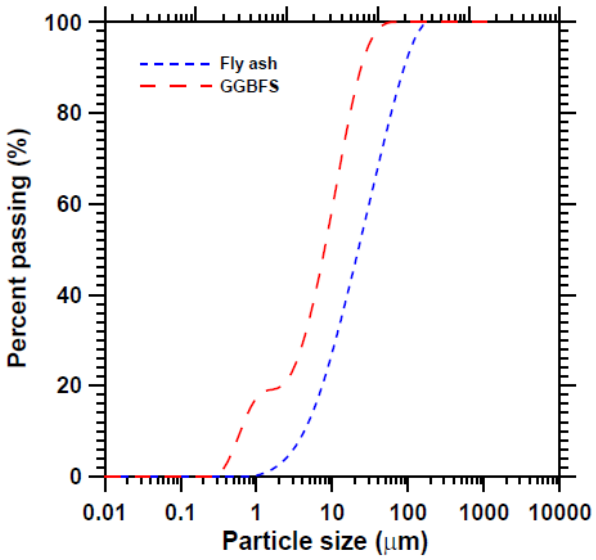

Figure 3-2: Particle size distribution of fly ash and slag (Ravikumar, 2012)

Fly ash and slag particle morphologies obtained using scanning electron microscopy is shown in Figure 3.3 (a) and (b) respectively. Fly ash has smooth spherical particles whereas slag is composed of angular particles of varying sizes.

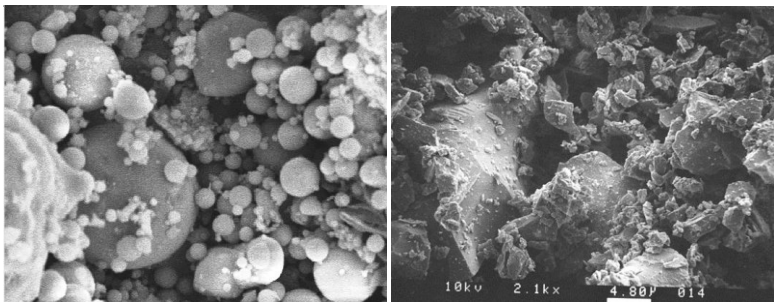

(a) (b)

Figure 3-3: Scanning electron micrograph of: a) fly ash and b) slag (PCA, 2003)

3.2. Activator Parameters (M, *n* and M_s)

The activation parameters used in this study are the Na_2O-to-binder ratio (*n*) and the SiO_2-to-Na_2O ratio (known as the silica modulus, M_s), and the solution concentration in terms of molarity (M) for sodium hydroxide activating solutions. The binders comprise of fly ash or slag (or both in the case of the blends). The ratio *n* provides the total amount of R_2O (where R is either Na or K) in the mixture, while the M_s dictates the proportion of alkali hydroxides and alkali-silicates in the activator. Thus, the total alkali contents are adjusted using the *n* parameter, for which several values were used in Chapter 4.

The activating agents used in Chapter 4 were sodium silicate solutions (waterglass) with a mass-based M_s ratio of 3.26 and a solids content of 40% and sodium hydroxide solutions. In Chapter 5, powder activators were used in the form of potassium silicate (Kasolv) or G-sodium silicate (G-SS) (both of these are commercial names, and are products marketed by PQ Corporation) with a mole-based M_s of 2.51 and 3.32 respectively. Since previous studies have shown that such high M_s values are not effective in activation of fly ashes (Chithiraputhiran & Neithalath, 2013; Ravikumar & Neithalath, 2012), reagent grade NaOH or KOH were added to the alkali-silicates to reduce their M_s values.

For example, if a mixture containing 1000g of binders was to be prepared with an *n* value of 0.05 and an M_s of 1.5, 50 g of Na_2O and 75 g of SiO_2 will be required. If waterglass was being used as the source of silica in the activator solution, 75 g of SiO_2 can be acquired using 245 g of waterglass, which contains 98 g of dissolved sodium silicate powder with a mass-based M_s ratio of 3.26. The waterglass also provides 23 g of Na_2O, and the remaining 27 g will be obtained with the addition of NaOH. Table 3-2

shows the mixture proportions used for 1000 g of binders with the activation parameters n of 0.03, 0.05 and 0.065 with two different M_s ratios (1.5 and 2). A liquid-to-powder ratio (l/p) of 0.35 was used, where the liquid consisted of the water added, the liquid proportion of waterglass (60%) and water generated in the dissociation of the alkali-hydroxide. The powders consisted of the binders, the solid fraction of waterglass and the Na_2O from NaOH.

Table 3-2: Sample mixture proportions for 1000g of binders for n values of 0.03, 0.05 and 0.065 and M_s values of 1.5 and 2

n	M_s	Binder	Waterglass (g)	NaOH (g)	Water (g)
0.03	2	1000	196.01	14.96	260.53
	1.5	1000	147.01	20.9	283.34
0.05	2	1000	326.69	24.94	200.88
	1.5	1000	245.02	34.83	238.90
0.065	2	1000	424.69	32.42	156.14
	1.5	1000	318.52	45.28	205.58

The powder activated samples were prepared a similar way; however the liquid consisted only of added water and water generated in the dissociation of the alkali-hydroxide.

Analytic reagent grade sodium hydroxide was used to prepare the alkaline NaOH activating solutions having concentrations of 6M and 8M. Activating solution-to-binding material ratios (a/b) were employed in the preparation of these samples. For example, to create 1000 ml of solution with a concentration of 6M, 240g of NaOH is required.

3.3. Mixing Procedure

3.3.1. Liquid activated systems

In the liquid activated systems using waterglass the NaOH solution used to reduce the activator M_s was prepared by dissolving NaOH beads in water and added to the required amount of water glass. For NaOH activated samples, the required amount of NaOH was first weighed into a measuring cylinder into which the required volume of water was added. For both cases resulting solution was then allowed to cool down to the room temperature for about 2 hours. A l/p ratio of 0.35 was used for all waterglass activated systems and an a/b ratio of 0.3 and 0.35 was used for NaOH activated systems.

River sand (d_{50} of 0.6 mm) was used as the fine aggregate. The mortar mixtures were proportioned to contain a sand volume of approximately 40±2%. Fly ash and the fine aggregates were dry-mixed thoroughly in a laboratory mixer. Requisite amount of the alkaline activator solution of the chosen concentration was gradually added while mixing until the components were homogenized. The mortar was filled in cubical acrylic molds of 50 mm size, and compacted using a table vibrator. Corresponding paste mixtures were also prepared for thermal analysis and spectroscopic studies.

3.3.2. Powder activated systems

In the powder activated systems using powder sodium and potassium silicates, a sand volume of 43±1% was used as the fine aggregate. The calculated amounts of binders (slag or both fly ash and slag); fine aggregate and activating powders were first dry-mixed thoroughly in a laboratory mixer. The required amount of water was then added to the starting materials to prepare the mortars and mixed for approximately 2

minutes until a homogenous mixture is obtained. The mixtures were then cast in 50 mm cube molds for compressive testing and porosity measurements. Corresponding paste mixtures were also prepared for spectroscopic and conductivity studies. For calorimetric studies, mortar mixtures were used as soon as they were prepared. A l/p ratio of 0.4 was used for these mixtures.

3.4. Curing Conditions

3.4.1. Heat cured samples

The specimens were cured for 24±1 h in the molds at 23±2°C in a covered state, demolded, and then subjected to the heat curing regime. Heat curing was carried out in a laboratory oven at 75°C for 48 h after the initial 24 h curing at ambient conditions based on a previous study (Somaratna, et al., 2010). Two batches were made for each of the mixture proportions to assess the effect of sealed and unsealed conditions on mechanical and microstructural properties. For the sealed samples, parchment paper and aluminum foil were used to seal the specimens.

A few specimens from both the NaOH and waterglass activated samples, based on the mechanical properties attained by the conditions described in the previous paragraph, were prepared again to be tested under shorter curing conditions to examine the significance of subjecting the specimens to heat immediately after casting (the specimens described earlier were left at ambient conditions for 24 h before heat curing started). These samples, immediately after casting, were inserted into a laboratory oven to undergo heat curing for 3h at 45°C or 75°C, removed for demolding and then reinserted into the oven for further heat curing. Samples initially heated at 45°C were subject to further

heating at 75°C for an additional 24 h, whilst samples initially heated at 75°C were reinserted into the oven at 75°C to complete the 24 h period. Figure 3-4 displays the various heat curing regimes with respect to curing times and temperature.

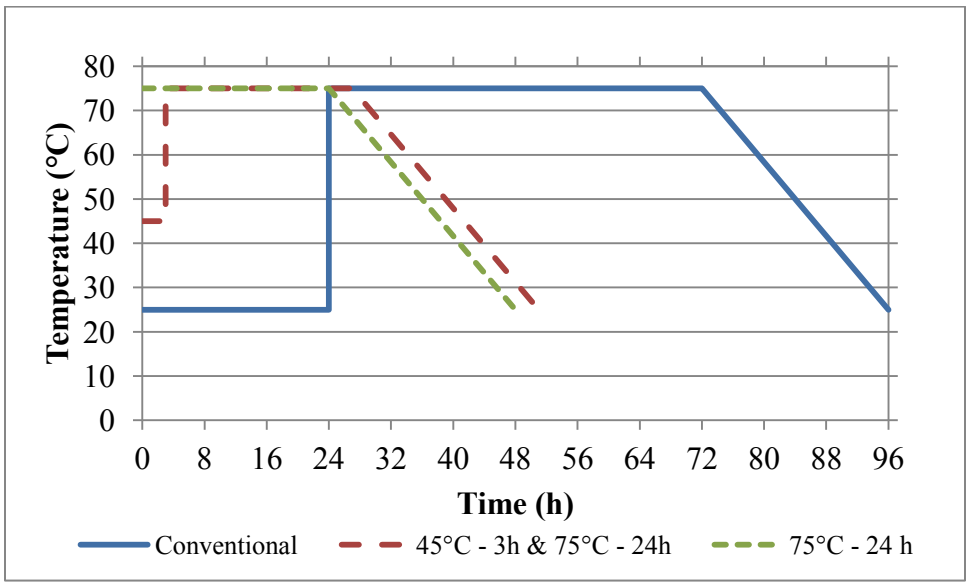

Figure 3-4: Curing time versus temperature for heat cured samples

3.4.2. Microwave cured samples

Microwave curing was started after 24 h of ambient curing, since microwave curing in the first 24 h was not possible due to difficulties in subjecting the mold material to microwave radiations for extended periods of time. For this reason, only the waterglass activated mortar with an n value of 0.05 and M_s of 1.5 was chosen since it reached initial set faster than the other mixtures.

The average incident microwave power of the oven used was tunable from 0 to 1200 W, at increments of 10%, and the microwave frequency used was 2.45 GHz. Three 50 mm cubical specimens were kept in the microwave cavity (37.5cm × 37.5cm × 25cm) for curing. Two batches of each of the mixture were made to assess the effect of sealed

and unsealed conditions on microwave curing. Sealing of the samples was done using parchment paper and plastic wrap. Previous studies have shown that at higher incident power levels (1200 W and 600 W) leads to severe cracking and deterioration of the specimens within a few minutes in the microwave (Somaratna, et al., 2010). It is possible that the temperature of a local area increases rapidly under non-uniform fields, resulting in "thermal runaway", leading to very high internal stresses and material fracture (Somaratna, et al., 2010). At shorter curing durations, no specimen cracking was observed when the specimens were subjected to a power level of 360 W. Hence an average incident power level of 360 W (corresponding to 30% of the maximum rated power) was used for most of the experiments reported here. However, at longer time periods, the specimens showed severe cracking and rupture (specifically for the unsealed samples). For this reason, samples were re-tested under both sealed and unsealed conditions at a lower power level of 240 W. The microwave curing duration was limited to a maximum of 120 min based on the observed results.

3.4.3. Combination heat curing and microwave curing

While heat curing (Criado, et al., 2010; Criado, et al., 2005; Kovalchuk, et al., 2007) and microwave curing (Somaratna, et al., 2010) have been shown individually to impact the property development in activated fly ash mortars, it is instructive to examine the combined effects of these curing methods from a viewpoint of potential energy and time savings. Selected samples activated using NaOH and waterglass were examined under a combination of heat and microwave curing regimes. Similar to the samples subjected to heat curing for shorter durations, these samples were also initially subjected

to 3h of heat curing at 75°C, after which they were removed for demolding and then underwent microwave curing at durations of 60min, 90min and 120min. Two batches of each of the mixtures were made to assess the effects of sealed and unsealed conditions. In order to prevent drying shrinkage of mortars at very early ages when heat cured, both the sets of samples were sealed during the short period in the oven.

3.5. Moist curing

For binders containing a calcium source (slag or fly ash-slag blends), the samples were subjected to moist curing at 23±2°C and a relative humidity > 98%. The samples were covered in plastic prior to placing in the moist curing chamber to prevent ponding on the surface of the samples. These samples did not undergo any heat or microwave curing regimes.

3.6. Early Age Tests

3.6.1. Isothermal calorimetry

Isothermal calorimetry has been found to be a useful technique to investigate the hydration of cementitious systems (Wadsö, 2003). Isothermal calorimetry is typically used to investigate the main hydration peak that occurs during the acceleration phase of the hydration process. The experiments in this study were carried out in accordance with ASTM C 1679 using a Calmetrix ICal 8000 isothermal calorimeter. The mortar mixtures were prepared using the same methods described in Section 3.3 and poured into the cups at constant mass (200 g) immediately before they were loaded into the isothermal calorimeter. The time elapsed between the water addition and sample loading was

approximately 4 minutes. The tests were run for 72-96 hours with the calorimeter temperature set to 25°C. Figure 3-5 show the isothermal calorimeter used for this study.

Figure 3-5: Calmetrix ICal 8000 Isothermal Calorimeter

3.7. Hardened Mortar Tests

3.7.1. Determination of compressive strength

The compressive strengths of the pastes and mortars were determined in accordance with ASTM C 109. The compressive strengths of the alkali activated cubes at several ages were determined by testing at least three specimens from each mixture at the desired ages. Heat and microwave cured cubes were returned to room temperature by cooling overnight prior to testing. Moist-cured specimens were tested at the respective ages after a few hours of drying at ambient conditions.

3.7.2. Determination of sample porosity using vacuum saturation method

The porosity of the mortar samples was determined by the vacuum saturation method as described in RILEM CPC 11.3 (RILEM TC, 1994). The samples were first dried at 105 ± 2°C until they reached a constant weight (m_1). The specimens were then allowed to cool and placed dry in a vacuum chamber for 2 hours under vacuum, followed by total submersion in water for an additional 4 hours under vacuum, followed by continued total submersion in water for 24 hours without vacuum. The saturated surface-dry weight (m_2) was then determined. The void ratio was calculated using the following equation:

$$VR\% = \frac{m_1 - m_2}{m_2} \times 100 \qquad \textbf{(3.7.2-1)}$$

3.7.3. Electrical solution conductivity tests

In order to capture the leaching effects of the unreacted ions (Na^+ or K^+, OH^- and Ca^{2+}) within the pore solutions of the specimens, the paste samples were placed in 200 ml of deionized water for an extended period of time after 7 days of moist-curing. Electrical conductivity measurements of the deionized water in which the alkali activated specimens were stored for several days were conducted. Figure 3-6 shows the conductivity meter (Mettler Toledo) used to measure the conductivity of the solution containing the sample.

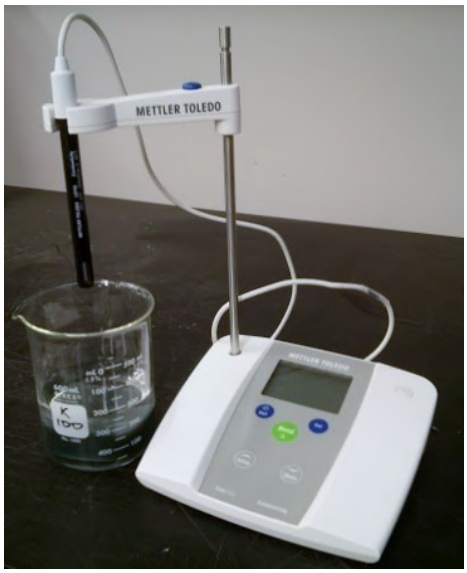

Figure 3-6: Mettler Toledo conductivity meter with the sample

3.8. Reaction Product Analysis

3.8.1. Fourier transform infrared spectroscopy

Attenuated Total Reflectance - Fourier Transform Infrared Spectroscopy (ATR-FTIR) allows for the determination of transmission spectra without destructive sample preparation. Spectra are obtained from the absorption or transmittance of a wave which is transmitted through an internal reflection element (IRE) of high refractive index and penetrates a short distance into the sample, in contact with the IRE. The IRE used was a diamond, selected because of its resistance to high pH and abrasion from sample removal and cleaning. A picture of the ATR attachment along with a schematic diagram of the beam path through the apparatus is shown in Figure 3-7.

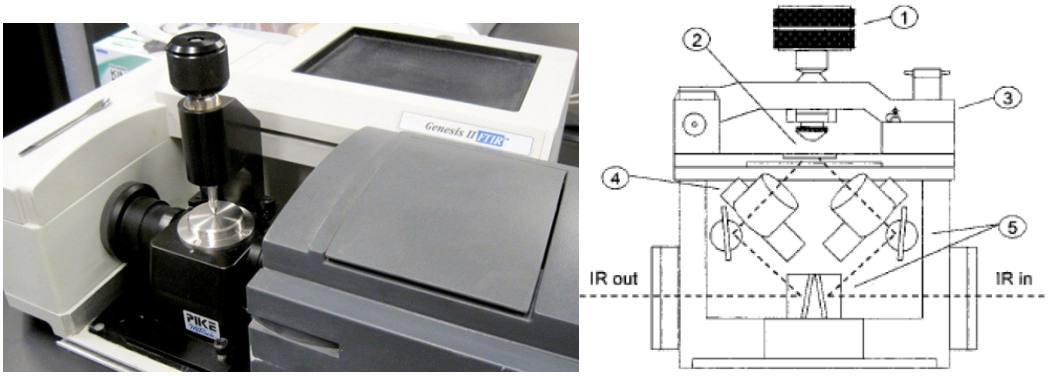

(a) (b)

Figure 3-7: a) ATR attachment with diamond crystal, (b). Schematic diagram showing the beam path through the ATR (1) torque head screw with limiter screw; (2) ATR crystal, (3) clamp bridge, (4) lens barrel, (5) mirrors (Tuchbreiter, et al., 2001)

3.8.2. Thermogravimetric analysis

Thermogravimetric analysis (TGA) is a useful laboratory tool used for material characterization. It is a technique in which the mass of a substance is monitored as a function of temperature or time as the sample specimen is subjected to a controlled temperature program in a controlled atmosphere (PerkinElmer, 2010). The basic principle of TGA is that as a sample is heated, its mass changes. This change can be used to determine the composition of a material or its thermal stability, up to 1000°C. Usually, a sample loses weight as it is heated up due to decomposition, reduction, or evaporation. A sample could also gain weight due to oxidation or absorption. The TGA equipment tracks the change in weight of the sample via a microgram balance. Temperature is monitored via a thermocouple. TGA data is usually graphed as weight percent vs. temperature (°C). TGA output curves can be analyzed in a number of ways. If the material in question is stoichiometric, the molar weight of the component being burned off can be ascertained

based on the weight percent lost and the total molar weight of the material (Iowa State University of Science and Technology, n.d.). TGA was carried out on representative samples obtained both from the core and the surface of the paste cubes so as to assess the effects of carbonation of the heat cured fly ash samples (Chapter 4) using the Perkin Elmer STA 6000. A heating rate of 15°C/min, and a temperature range from ambient to 995°C was used for the thermal analysis studies. A picture of the TGA equipment used in this study is shown in Figure 3-8.

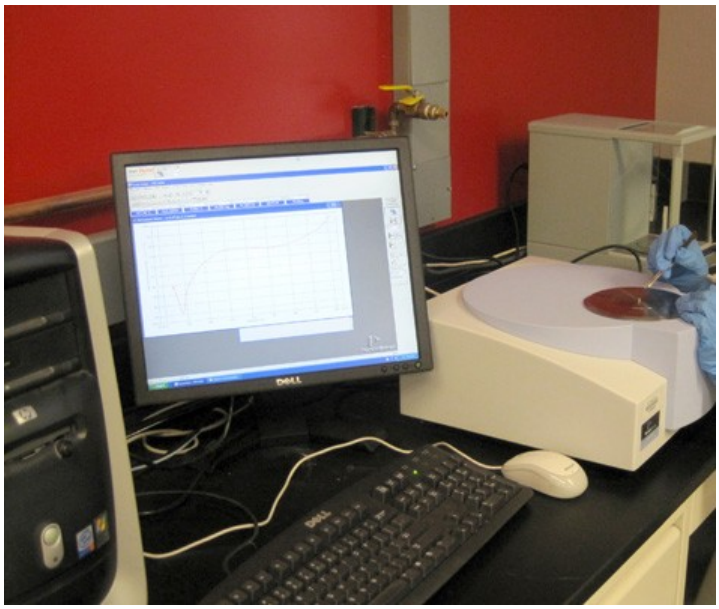

Figure 3-8: Perkin Elmer STA 6000 equipment set up

Chapter 4

INFLUENCE OF THERMAL CURING ON STRENGTH AND REACTION PRODUCTS OF NAOH AND SODIUM SILICATE ACTIVATED FLY ASH

The process of alkali activation of fly ash causes the dissolution of its glassy components, allowing for the formation of aluminosilicate gels that are responsible for beneficial mechanical and durability properties. This chapter explores the influence of curing conditions on the mechanical and microstructural properties of the reaction product formed.

4.1. Influence of Heat Curing on Compressive Strength

4.1.1. Waterglass activated samples

Figure 4-1 shows the compressive strengths as a function of the n and M_s values of waterglass activated fly ash mortars that were heat cured at 75^{o}C for 48 h after 24 h at ambient temperatures, under sealed and unsealed conditions. The compressive strengths follow expected trends, with a higher strength being observed when the n value is increased. Between an n value of 0.03 and 0.05, there is a significant increase in strength, attributable to the increased alkalinity that improves the dissociation of fly ash. While lower M_s values (or higher free Na_2O content in the activator) is beneficial at an n value of 0.05, the activator M_s becomes quite insignificant at higher n values because of the higher total Na_2O content.

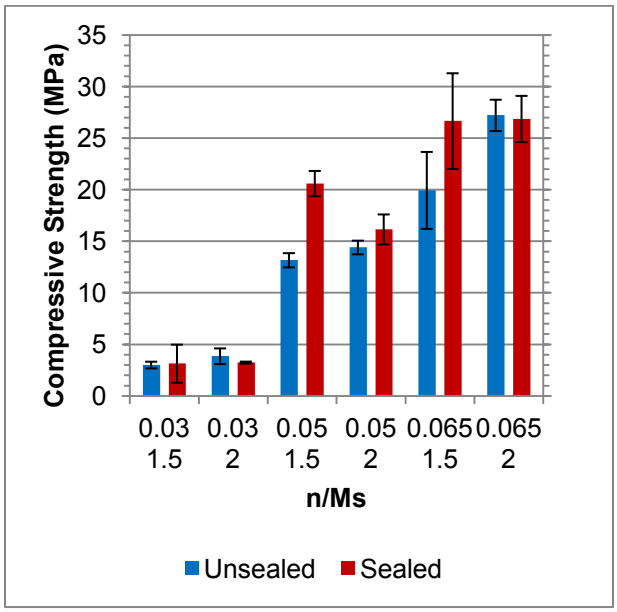

Figure 4-1: Comparison of compressive strength of heat cured (75°C for 48 h) sealed and unsealed waterglass activated mortars with respect to n and M_s values. Errors bar indicate one standard deviation of the mean compressive strength of the three companion species

The samples activated under sealed conditions generally exhibit higher strengths. The reason for unsealed specimens demonstrating lower compressive strengths is possibly due to carbonation (note that, as the diffusion coefficient of CO_2 in air is ten times higher than that in water (Verbeck, 1958), carbonation is more likely under unsealed conditions). Carbon dioxide is an agent that can drastically affect the long-term durability of concrete structures. It is of particular concern in alkali activated binders as these materials present a potentially higher susceptibility to carbonation compared to conventional cements (Bernal, et al., 2011). Carbonation lowers the pH of the system causing significant reductions in Si dissolution and a persistence of a high Al content. These conditions have a greater effect on silicate rather than aluminate species, since Al dissolves more readily than Si in the alkaline medium. The resulting reaction product is

reported to be granular and porous, and thus results in a weaker material (Criado, et al., 2010). Hence, carbonation can only be prevented by subjecting the sample to high levels of humidity throughout the curing process (Criado, et al., 2010). By sealing the samples during the curing process, the mixing water supply for the samples was effectively trapped since evaporation is prevented. The availability of water and the high pH of the system facilitated by the lack of carbonation under sealed conditions favors dissolution of the glassy component of the fly ash. Through the increased amounts of reactive free water, ion movement can continue for longer durations allowing for increased ash activation, thus intensifying the Si polymerization of the initially Al rich material and resulting in a dense and compact end product. (Kovalchuk, et al., 2007)

It is also generally noticed that the sealed curing has a greater influence on strength at lower M_s values than it does at higher M_s values. This behavior is attributed to the higher anion (OH^-) concentration from the added NaOH to maintain required n values allows for increased dissolution of the original fly ash matrix, which results in enhanced ash activation and thus the compressive strengths.

The curing conditions do not affect samples activated with the highest n and M_s ratios (e.g. 0.065 and 2 respectively), as they contain high amounts of reactive ions and soluble silica to obtain favorable compressive strengths, thereby minimizing the influence of water retained during the curing process. In these situations, the unsealed samples are likely subjected to slightly higher temperatures due to the lack of the sealed barrier and hence results in increased fly ash activation. However, the consequence of these high n and M_s values are the excessive amounts of leaching of ions from the pore solution during the curing process causing the samples to shrink exceedingly. Previous studies have

found that the optimal n and M_s values for fly ash activation is 0.05 and 1.5 respectively (Chithiraputhiran, 2012; Wang & Scrivener, 1995; Chithiraputhiran & Neithalath, 2013).

4.1.2. NaOH activated samples

Figure 4-2 demonstrates the compressive strength of mortar samples activated using NaOH solutions cured under sealed and unsealed conditions. A higher NaOH concentration results in increased strengths as shown in this figure. It can also be noticed that an increase in the activator-to-binder ratio (a/b) decreases the compressive strengths even though the availability of ionic species responsible for activation is higher in the case of the higher a/b mixtures. This shows that higher porosity resulting from the higher a/b is more important from a strength viewpoint, which has been shown before (Ravikumar, et al., 2010).

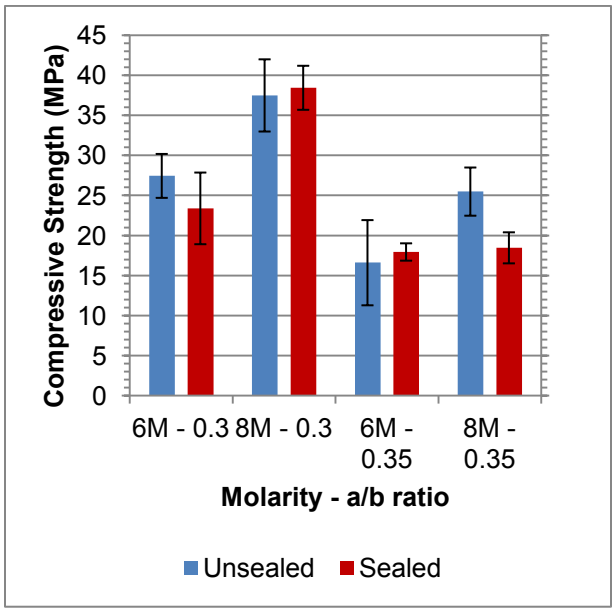

Figure 4-2: Comparison of compressive strength of heat cured (75°C for 48 h) sealed and unsealed NaOH activated mortars with respect to molarity of solution and activator-to-binder ratio . Errors bar indicate one standard deviation of the mean compressive strength of the three companion species

For the NaOH activated samples, the strengths are generally independent of whether the samples were sealed or not, which is in contrast to the sodium silicate activated samples where sealed curing was observed to be more effective as shown in Figure 4-1. This can possibly be explained by the Al dissolving more readily than Si when carbonation occurs, which causes greater precipitation of the Al rich sodium aluminosilicate hydrate (N-A-S-H) gel whose Si content barely varies over time since the reduced pH level due to carbonation hinders further Si dissolution (Criado, et al., 2005). In other words, carbonation does not adversely influence the strength of NaOH activated fly ash mixtures. In the sealed condition, where the pores are saturated, the Si preferentially reacts over the Al to form the secondary gel; however not enough time has elapsed for the formation to conclude resulting in slightly weaker strengths. Thus, dry curing is only recommended for NaOH-based systems (i.e. systems with low SiO_2/Al_2O_3 ratio).

4.1.3. Effects of heat curing at early ages

Figure 4-3 compares the compressive strengths obtained using alternative heat curing regimes where the specimens are heat treated for lower curing durations immediately after casting to those obtained through heating after 24 h in ambient conditions for both NaOH and waterglass activated samples. Studies have found that the rate of strength gain is rapid up to 24 hours of curing time, beyond which the strength gain is only moderate (Skvara, n.d.), allowing for the potential to lower the heat-curing duration and cut back on energy costs. This curing type was implemented for only two mixes at various curing times.

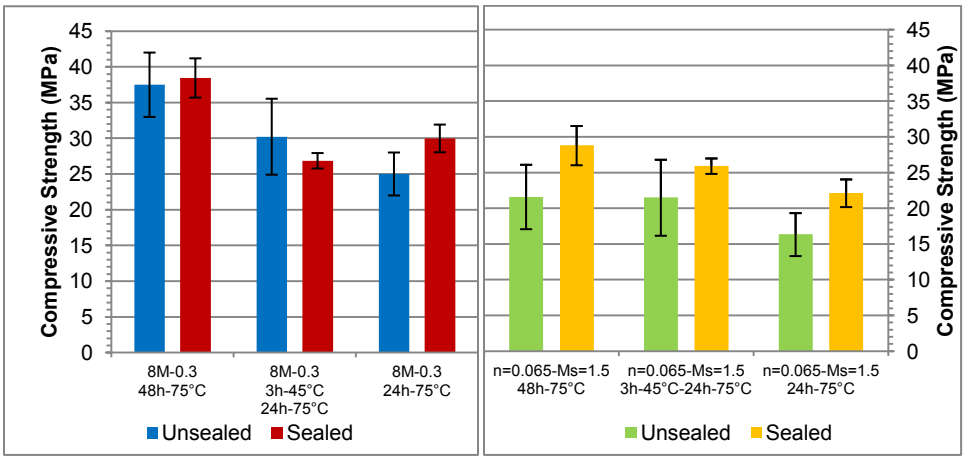

Figure 4-3: Comparison of compressive strength of heat cured sealed and unsealed samples of NaOH and waterglass activated mortars with respect to curing time and temperature. Errors bar indicate one standard deviation of the mean compressive strength of the three companion species

For samples activated with NaOH solutions, it can be seen that the end products do not reach the same level of compressive strength as those cured using heat curing durations described above, particularly for unsealed samples. Delaying the heat-curing application, therefore does not significantly affect the peak strength gain (Ravikumar, 2012). Once again, there is no meaningful trend visible for the effects of sealing the sample for the mixes activated using NaOH.

For samples activated using waterglass, curing immediately after casting does prove to be somewhat more effective for reaching reasonable compressive strengths. For unsealed samples, the extra 3 hours at 45°C allows for significant improvements with strengths, reaching the same levels as those attained by the heat-curing techniques described above, even when the total curing duration was lower (previous was 24 h at ambient temperatures + 48 h at 75°C). The effect of sealed curing follows the same trends as those described in Section 4, with the reduction of carbonation and increased

mixing water supply resulting in more favorable mechanical properties. Thus, sealed curing under this alternate heat curing regime comes very close, and can potentially surpass the strengths attained by heat curing using the standard methods described in previously if allowed to be exposed to heat curing for longer durations.

4.2. Influence of Microwave Curing on Compressive Strength

Figure 4-4 shows the compressive strength as a function of curing duration of waterglass activated fly ash mortars cured using microwave radiation. Until 60-90 min of microwave curing, increased curing times result in increased strengths. Microwave radiation provides volumetric heating of the sample through interactions at the molecular level with the electromagnetic field (Somaratna, et al., 2010). Microwave-material interactions result in translational motions of the free or bound charges and the rotation of dipoles. The inertial, elastic and frictional forces that resist these motions causes volumetric heating of the material. Since the microwave curing is predominantly contingent upon energy conversion rather than heat transfer without relying on heating from the surface, rapid and uniform heating is possible (Somaratna, et al., 2010). As a result, the formation of N-A-S-H gel is enhanced, resulting in faster strength development.

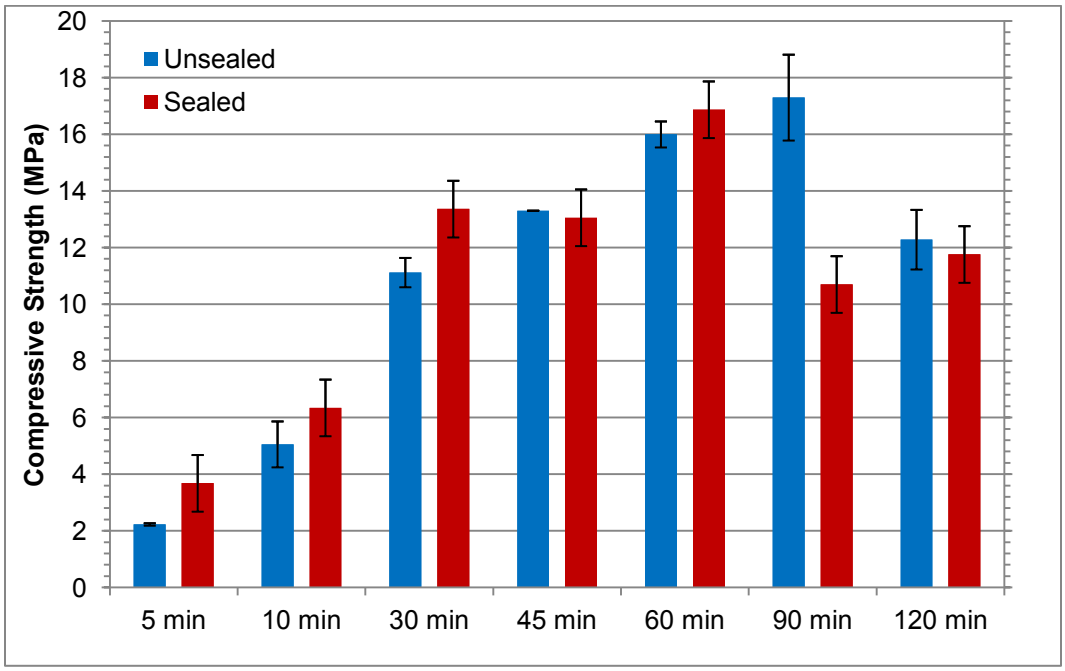

Figure 4-4: Comparison of compressive strength of microwave cured sealed and unsealed waterglass activated mortars at 360 W with respect to curing durations

However, with the power level set to 360 W, after about 45 min of heat curing, there is a significant drop in compressive strength. Figure 4-5 shows the temperature development of the samples as a function of microwave curing duration. A gradual peak can be observed until 45 min, after which there is a drop. This can be attributed to the complete evaporation of all free water within the specimen. Excess of microwave heating beyond this point results in a decay of the sample microstructure caused by the removal of bound water at temperatures in excess of 100^{o}C; thus resulting in the loss of compressive strength as indicated by Figure 4-4 at curing durations beyond 60 min for sealed samples and 90 min for unsealed samples. However, the compressive strength attained after 60-90 min of microwaving curing nevertheless surpasses the compressive strength of unsealed heat cured samples activated with the same parameters.

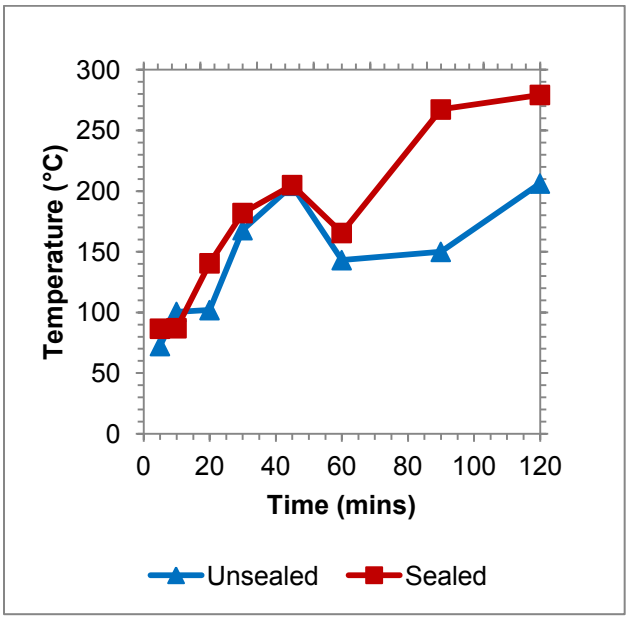

Figure 4-5: Surface temperature of specimens after microwave curing with respect to curing duration

The energy absorbed by a material is primarily due to the dielectric heating of the pore solution, thus a reduction in moisture content reduces the dielectric loss factor (Somaratna, et al., 2010). The moisture loss from the mortar cubes are accelerated by the increased temperatures, even though these high temperatures enhance reaction product formation and better strength gain.

The high specimen temperatures and the pronounced rate of moisture loss contribute to micro-cracking as trapped steam tries to escape, resulting in strength reduction. Sealing the samples during microwave radiation traps the water in the system, as evaporation of free water is prevented. However, this in turn traps heat since heating of the sample is primarily due to the heating of the pore solution, causing moisture loss to occur much faster. After 60 min there is a deterioration of the sample structure for sealed samples, whereas unsealed samples can withstand the radiation longer.

Figure 4-6 demonstrates the effects of microwave curing after reducing the power level to 240 W. This offers some improvement on the mechanical strength of the specimen, with samples reaching strengths as high as 19 MPa after only 90 min of microwave curing.

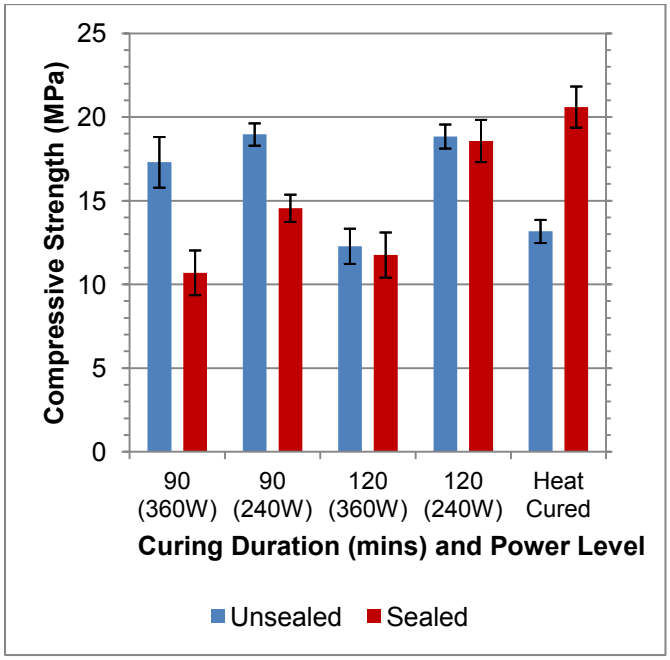

Figure 4-6: Comparison of compressive strength of sealed and unsealed waterglass activated mortars at various microwave power levels and heat curing

4.3. Combination of Heat Curing and Microwave Curing

Figure 4-7 displays the strengths obtained by the samples after heat curing for 3 hours at 75°C followed by 60, 90 and 120min of microwave curing. This combined curing method was utilized in an attempt to lower curing times and the amount of energy consumed, but maintaining peak strength gain

It is evident from the data in Figure 4-7 that there is no appreciable strength gain after 60 min of microwave curing. Instead, the excessive temperatures after microwave

curing for prolonged periods have a tendency to decay the microstructure and reduce mechanical strength (as experienced by prolonged curing at 360 W). This is because with increased starting temperature, the samples reach the critical temperature that causes deterioration much earlier.

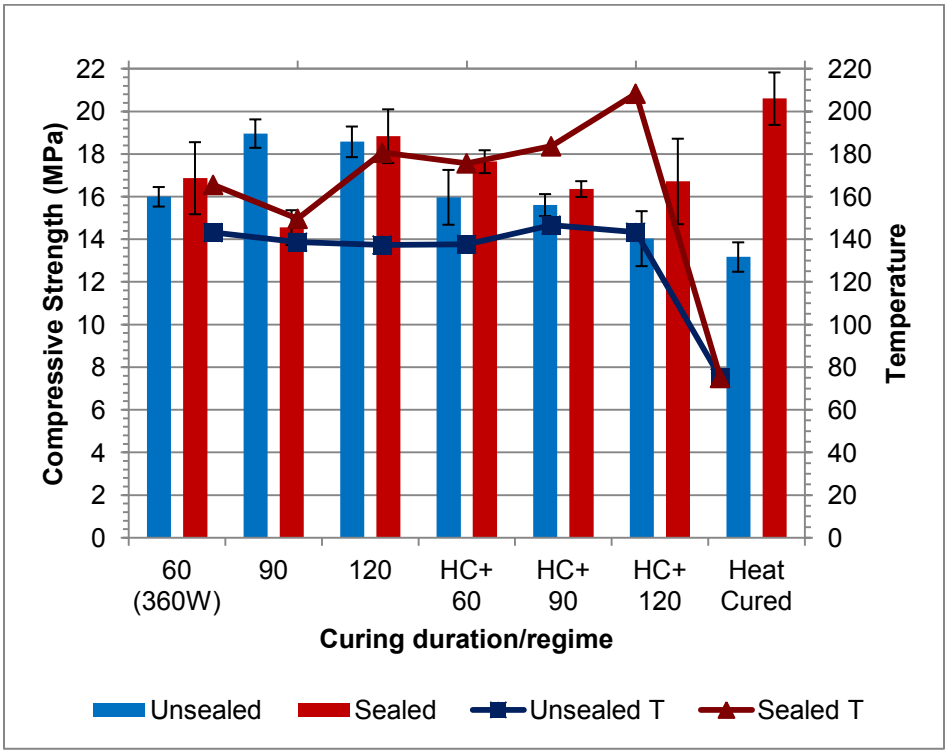

Figure 4-7: Comparison of compressive strength of sealed and unsealed waterglass activated mortars under various curing regimes. Microwave power level set to 240 W unless otherwise specified

Figure 4-8 plots the strength gain of the 8M NaOH samples through various curing methods. The same combined heat and microwave curing process was also used for 8M NaOH activated samples (which was the sample with the highest strength in the heat curing process). The conventional heat curing regime with 24 h at ambient

temperatures followed by 48 h of heat curing at 75°C continues to provide the highest strength, followed by combination of heat curing with 120min microwave curing.

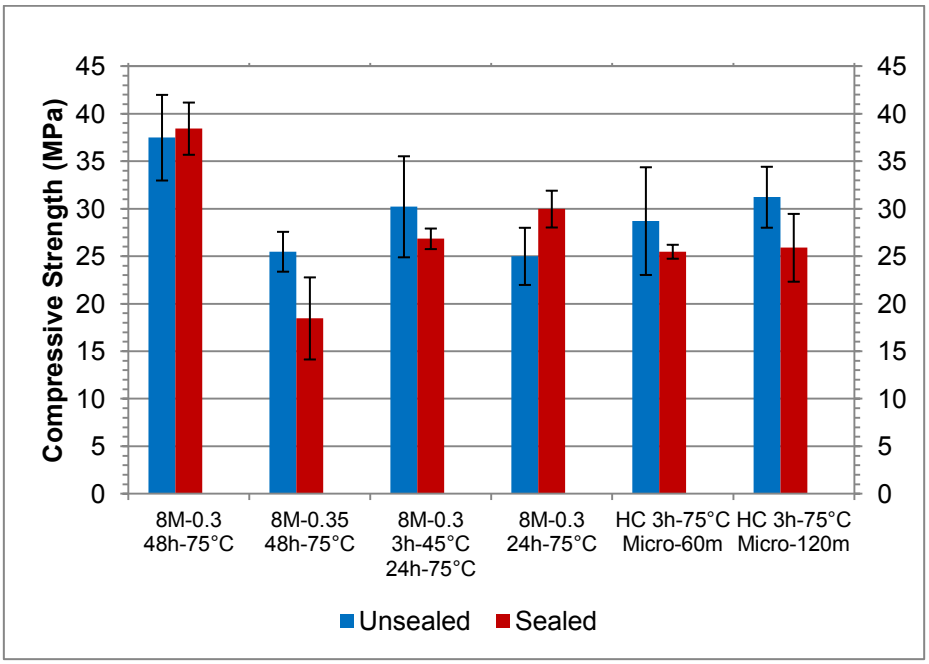

Figure 4-8: Comparison of compressive strength of sealed and unsealed 8M NaOH activated mortars at various curing regimes. Microwave power level set to 240 W

Figure 4-9 depicts the time vs. temperature plot of NaOH activated specimens. An interesting observation when comparing waterglass activated samples to NaOH activated samples is that after 60min of microwave curing, there is no significant temperature change of the samples activated by NaOH solution. This implies that microwave energy is not as effective in heating the dry solid (after all free water has evaporated) in samples with lower soluble Si content (Somaratna, et al., 2010).

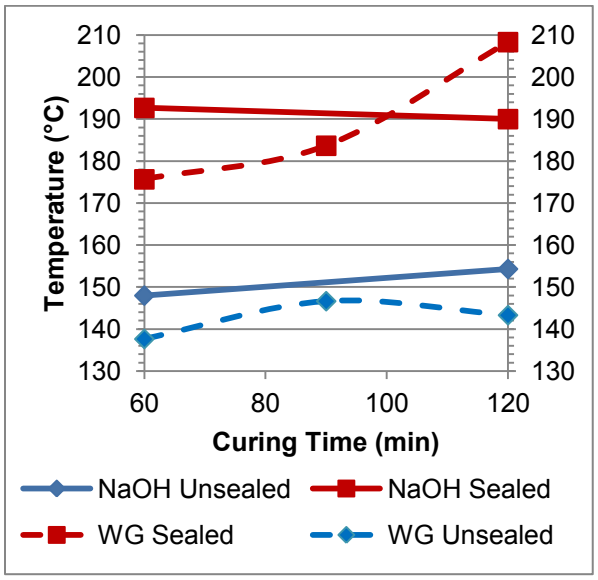

Figure 4-9: Curing time vs. temperature of 8M NaOH activated samples

4.4. Reaction Products

4.4.1. Thermogravimetric analysis (TGA)

It is quite evident from above sections that the sealed samples display more reaction product formation. When the material is sealed to prevent evaporation, the Si content of the initial Al-rich material gradually increases. When the samples are in direct contact with the atmosphere water loss and early age carbonation takes place, which results in a less polymerized gel. A certain amount of excess water is needed to dissolve aluminate and silicate species to allow them to be taken up in the aqueous phase for N-A-S-H gel precipitation, as described previously. When the amount of liquid is limited, the dissolution of the vitreous component of the fly ash is retarded.

The structure of the TGA curve roughly follows that of OPC pastes, where the initial mass loss is attributed to the loss of free water in the system, which represents the maximum mass lost. However, unlike OPC curves the TGA curves of fly ash lack certain

distinguishing features (such as peaks for C-S-H or CH). The next gradient change of the curve occurs at approximately 180°C, which can be attributed to the complete evaporation of all free and weakly adsorbed water in the system. From this point to approximately 600°C can be assumed to represent the dehydroxilation of N-A-S-H gel, where additional water mass is being evaporated from the nano-pores of the gel (Škvára, et al., 2009). Total dehydration of the gel occurs at 750-800°C (Škvára, et al., 2009; Bakharev, 2006). It should be emphasized that the TGA curves are of a smooth nature, with no significant peaks being observed (unlike TGA curves for OPC pastes). This is indicative of the absence of hydrated minerals in crystalline form, namely $Ca(OH)_2$, $CaCO_3$, or ettringite (Škvára, et al., 2009).

Figure 4-10 shows the thermal analysis curves of waterglass samples activated with the same parameters cured under various curing regimes. It is evident that there is very little free water remaining in the system for samples that undergo a microwave curing regime. This further verifies the importance of available water for reaction, explaining why the microwave samples do not reach the same strength as the sealed heat cured samples (which evidently contains a substantial amount of free water, represented by the slope between 50-180°C).

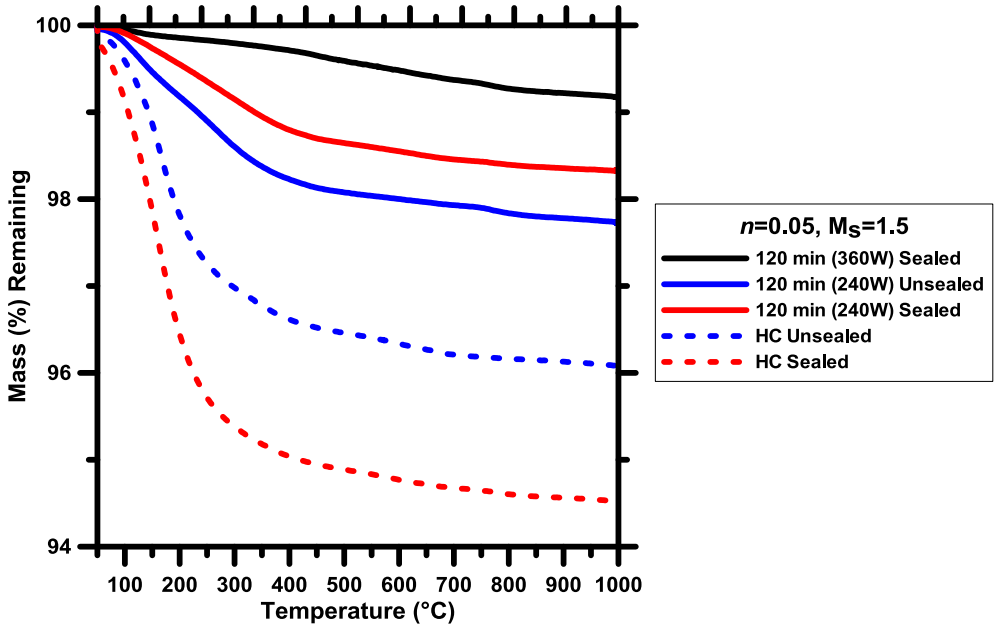

Figure 4-10: Comparison of TGA curves of samples with n value of 0.05 and Ms of 1.5 undergoing heat curing and microwave curing

Figure 4-11 shows the stoichiometric mass of N-A-S-H gel (based on its dehydration during the thermal analysis process). This was calculated by assuming a chemical composition of the resulting N-A-S-H as $3.03Na_2O{\cdot}3Al_2O_3{\cdot}5.25SiO_2{\cdot}7.5H_2O$. It needs to be remembered that this is an approximate stoichiometric composition and the actual values of Si/Al, Na/Al, and Na/Si would depend on the degree of reaction which in turn is a function of the activator and source material characteristics in addition to the thermal activation regime. This figure also depicts the same trends as the TGA curve with the heat cured samples showing the highest amount of gel formation, which can again be attributed to the availability of free water for the reaction process to continue. Also of importance are the relatively low amounts of N-A-S-H gel in these mixtures. Since N-A-S-H is formed as a layer around the fly ash particles, further reaction becomes diffusion controlled. The dense gel around the fly ash particles slows down the reaction

further, and typically in thermally processed systems, only a small amount of gel can be expected, as shown here.

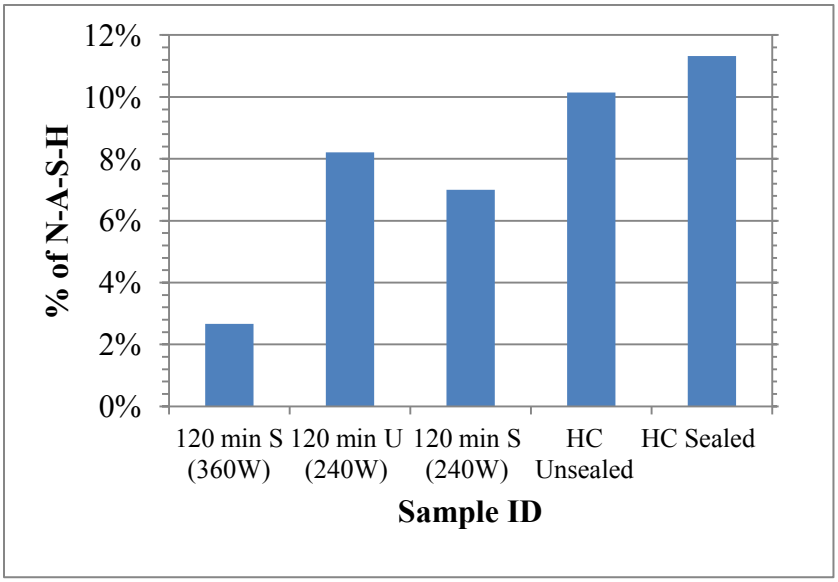

Figure 4-11: Mass of NASH gel lost during TGA testing

4.4.2. Analysis of the chemical structure using FTIR

In the alkali activation of fly ash, the main peaks of consideration during infrared studies of the various matrices are those associated with the bending and stretching modes of the main T-O bonds (where T is either Si or Al) that form the backbone of all aluminosilicate structures (van Jaarsveld & van Deventer, 1999; Lemougna, et al., 2011). The peaks that occur between 950 cm^{-1} and 1050 cm^{-1} are attributed to asymmetric stretching of T-O bonds. The vibrations logged within these regions are considered to originate from within the Si and Al tetrahedra that are the main building blocks of the N-A-S-H gel (van Jaarsveld & van Deventer, 1999). Other bands occurring at approximately 1400 cm^{-1} have been associated with sodium carbonate. The peaks detected between 3310-3385 cm^{-1} and 1630-1655 cm^{-1} represent stretching and bending

modes of OH^- groups present in H_2O and the hydration products (Chithiraputhiran, 2012). The bands associated with the vibrations originating within the Al- and Si tertrahedra are indicative of the degree of polymerization that has taken place (Ortego, et al., 1991), where a higher degree of polymerization can be associated with higher wavenumbers.

Figure 4-12 compares the FTIR spectra of two samples activated using waterglass and NaOH. From the FTIR results, the wavenumbers produced from binders activated using only NaOH are not as high as those activated using waterglass. This indicates that the degree of silica polymerization is not as high and the gel formed is the intermediate, aluminum-rich phase. Increasing the curing time should lead to the creation of the more stable, silicon-rich gel product.

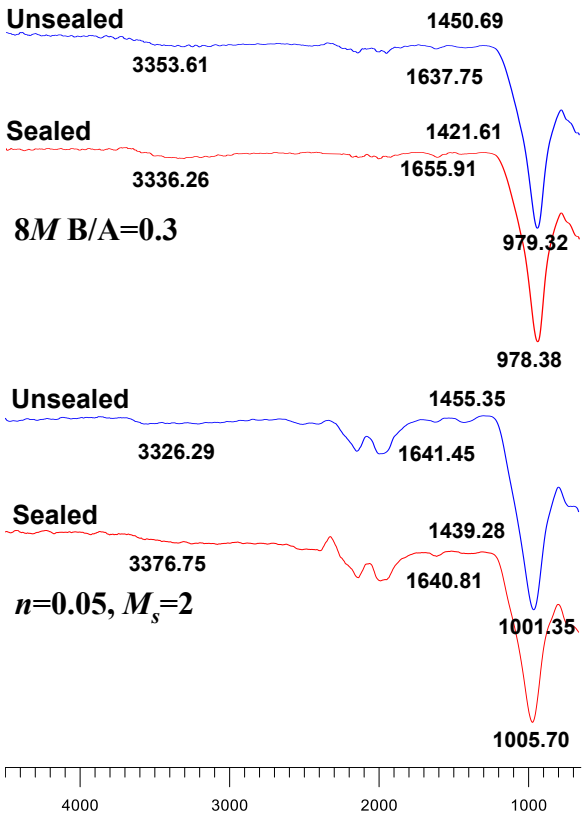

Figure 4-12: FTIR spectra of alkali activated fly ash pastes using NaOH and waterglass solutions under sealed and unsealed conditions

Without the presence of the soluble silica in the NaOH activated samples, the dissolution of fly ash is intensified, resulting in the lower wavenumbers of peaks in the FTIR spectra. This is because soluble silicates reduce alkali saturation in pore solution and promote greater interparticle bonding. Also, it has been found that higher percentages of the soluble silica in geopolymer system retards the dissolution of the ash material due to increased saturation of the ionic silica species and promotes precipitation of larger molecular species, resulting a stronger gel (Gel 2) with an enhanced density (Petermann, et al., 2010).

In addition, the position of the band depends on the Al/Si ratio of the reaction product. The substitution of a Si^{+4} for an Al^{+3} involves a reduction of the T-OT angle and therefore the appearance of the signal at a lower frequency, due to the smaller bonding force and the fact that the Al-O bond is longer than the Si-O bond (van Jaarsveld & van Deventer, 1999; Petermann, et al., 2010). This also contributes to why the wavenumbers for the stretching vibration of the T-O-T linkages in the FTIR spectra of NaOH activated samples are much lower than those activated with waterglass.

Figure 4-13 below exhibits a comparison of FTIR spectra of heat cured samples versus microwave cured samples activated with the same parameters. It is interesting to note that while the gel polymerization of the microwaved samples cured at 240 W does result in a higher polymerization of the gel structure (with wavenumbers reaching as high as 1001 cm^{-1}), this is not reflected in the compressive strengths (as shown in Figure 4-6). This illustrates the potential for the effectiveness of microwave curing over conventional

heat curing if the excessive temperatures that cause microcracking of the sample microstructure can be controlled.

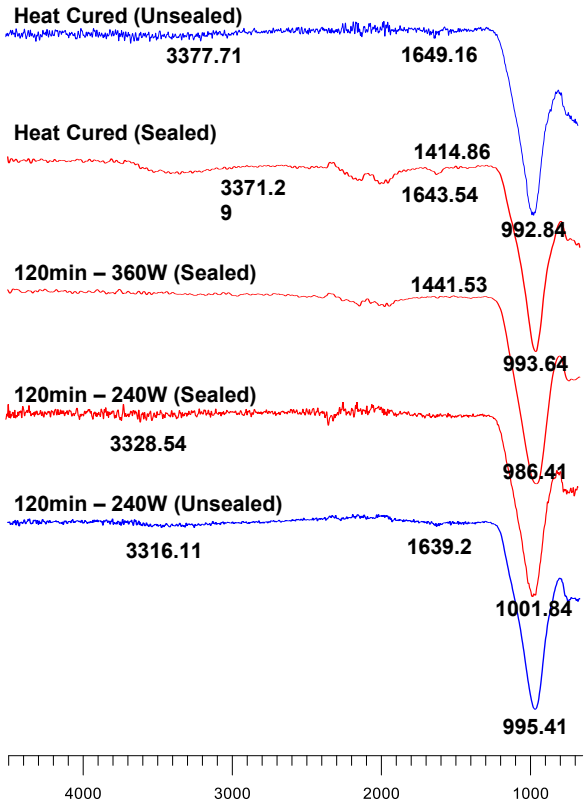

Figure 4-13: Comparison of FTIR plots of samples with n value of 0.05 and Ms of 1.5 undergoing heat curing and microwave curing

4.5. Summary

In this chapter, the various heat curing regimes available for the alkali activation of fly ash were explored. It was found that the samples cured using ordinary thermal curing techniques reached the highest peak strengths (up to 38.5 MPa). The effects of curing conditions were also investigated by sealing the samples to effectively trap the mixing water supply by preventing evaporation. The results showed that sealing the samples during the heat curing process results in earlier compressive strength gain for waterglass activated mixes, however did not have significant influence of NaOH activated mixes. FTIR spectroscopic analysis was used to confirm the degree of polymerization, with waterglass samples showing a shift to higher wavenumbers for sealed samples, indicating a higher degree of polymerization. Microwave curing was also explored as a replacement for traditional thermal curing techniques, which result in much faster compressive strength gain, although they did not reach the same peak strengths. The lack of strength gain for longer microwave curing durations was attributed to early moisture loss from the system and consequential microcracking, which was verified through the application of TGA studies.

Chapter 5

EFFECT OF ACTIVATOR CHARACTERISTICS ON THE REACTION PRODUCT FORMATION IN FLY ASH/SLAG BINDERS ACTIVATED USING ALKALI SILICATE POWDERS AND HYDROXIDES

The characteristics and type of the activating agent plays a significant role in determining the reaction rate and its extent, and also on the type of reaction products formed. This inherently affects the early- and later-age properties of the final binder system (Puertas, et al., 2004; Hajimohammadi, et al., 2011; Wang, et al., 1994). Alkali silicate solutions with different silicate modulus (M_s) have been extensively studied for their effectiveness in producing strong and durable binders under standard moist curing conditions, specifically for source materials containing reactive calcium (e.g. slag). However, from a practical standpoint, one of the most fundamental concerns relates to the handling of these caustic activator solutions. A potential alternative comes with the use of powder activators that are directly blended with the source material so that the handling hazards are substantially lowered. This also presents the opportunity to develop alkali activated systems that can be pre-packaged and requires the use of water alone to initiate the reaction, similar to that of OPC concretes, which likely will increase the commercial acceptability of these materials.

In this chapter, the mechanical properties of slag and fly ash-slag blends activated with sodium and potassium silicate powders and hydroxides are explored. Isothermal calorimetry is used to understand the effect of the activator characteristics, along with distinguishing the fundamental differences in early age reaction kinetics when powdered

form of sodium silicate and potassium silicate activators are utilized. The fundamental differences between the two types of powder activators mostly relate to the dissolution effects of the powder and are brought out through the use of FTIR spectroscopy, electrical conductivity and vacuum saturated water absorption measurements.

5.1 The Effect of Na^+ or K^+ as Alkaline Activators on Compressive Strength

Figure 5-1 below shows the compressive strength data of slag and fly ash-slag blends activated with sodium (Na) and potassium (K) silicates and hydroxide powders after 3, 7 and 28 days of curing. It is clearly evident that the binders activated using potassium performs better than those activated using sodium at later ages. This can be attributed to a number of reasons, namely the viscosity of the pastes, heat generated by the dissociation of the alkali activating powders into solution and the dissolution capabilities of the alkali activators.

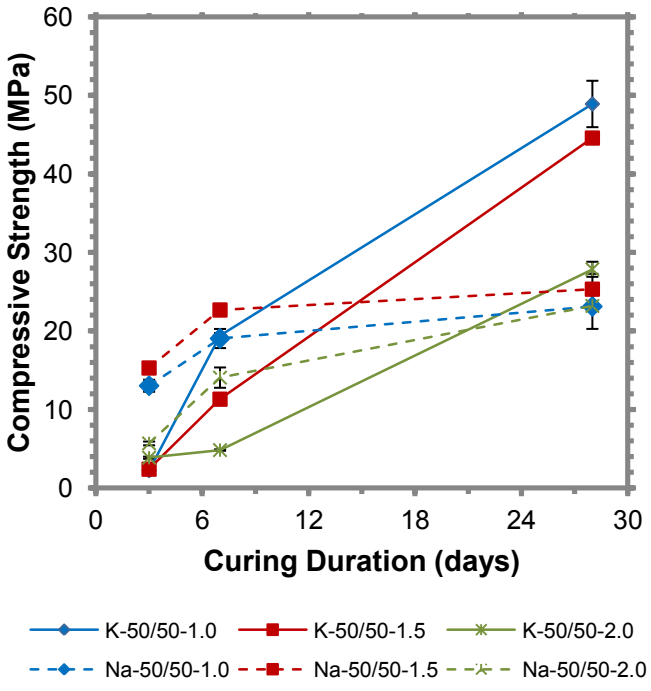

(a)

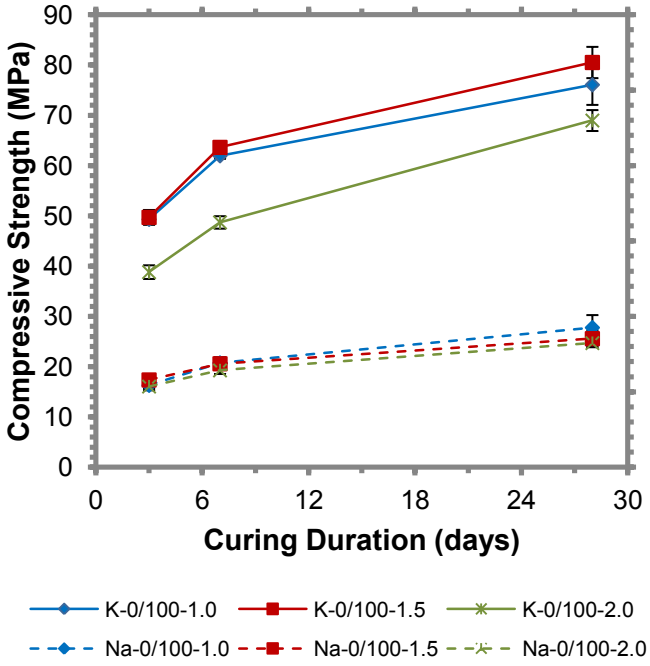

(b)

Figure 5-1: Compressive Strength of (a) 50% fly ash and slag blends and (b) 100% slag mortar mixes activated with sodium silicate and potassium silicate powders

Studies have found that K-based alkali activated binders tend to have a less porous and more homogenous structure than Na-based binders activated using the same activation parameters. This can be related to the fact that Na-based activation solutions and the resulting pastes are much more viscous and polymerize much faster, thus inhibiting long mixing durations, good homogenization and proper removal of entrapped air bubbles (Lizcano, et al., 2012). It has also been suggested that the decrease in viscosity of K-based pastes have been linked to potassium stabilizing larger silicate oligomers in solution with which $Al(OH)^{4-}$ prefers to bind (Komnitsas, et al., 2009) by forming cation-ion pairs with silicate oligomers more readily than sodium (Duxson, et al., 2005; Xu, et al., 2001), thus providing a denser network structure with enhanced mechanical properties. The sodium counterpart prefers ion pairing with the smaller

silicate monomers and dimers (Provis & van Deventer, 2007). Therefore, the dissolution of silicon might consume less water in potassium activated pastes, resulting in the lower viscosities (Duxson, et al., 2005). In solid-liquid systems with high viscosities, there may be areas of the material that have less water available during mixing, and thus do not react completely (Provis & van Deventer, 2007). This can also contribute to the less homogenous structure resulting in weaker compressive strengths of the Na-based systems in Figure 5-1.

The cation characteristics also play a significant role in the activation process. Since K^+ is more basic it allows for a higher rate of solubilized polymeric ionization and dissolution. In addition, the fact that K^+ a smaller solvated ion radius than Na^+ (r = 3.31 Å, vs. sodium's 3.58 Å) allows for a tendency of K-based activators to form a more dense and intimate polycondensation reaction which leads to greater overall network formation and an increase in the compressive strength of the matrix (Khale & Chaudhary, 2007; Phair & van Deventer, 2001; Provis & van Deventer, 2007; Bach, et al., 2013). This supports the trends shown in Figure 5-1.

The reaction products formed in the alkali activation of slag and fly ash-slag blends is predominantly C-S-H with a low Ca/Si ratio, at the very beginning of the reaction. The rest of the Ca may react with Al to form a phase separated Al-substituted calcium silica hydrate (C-(A)-S-H) (Li, et al., 2010). The C-(A)-S-H particle has a layered structure with four main layers and two interlayers as shown in Figure 5-2. Since the K^+ has a smaller solvated ion radius and lower enthalpy of hydration than sodium (-321 kJ/mol vs. -405 kJ/mol), it would exhibit a high affinity for the negatively charged surfaces of the C-(A)-S-H particle (due to the substitution of a Si^{4+} with an Al^{3+}). It can

also lose part of its solvation water and form inner-sphere complexes with the C-S-H sites. Also, due to its smaller size, it can penetrate into the interlayer, which sodium ions cannot. Thus, Na^+ only forms outer-sphere complexes on the external surface of the particle, whereas K^+ can potentially access more surface area by compensating the negative charges within the interlayer. (Bach, et al., 2013). The resultant network of the K-based systems will therefore be denser since the interlayer network can be filled more efficiently.

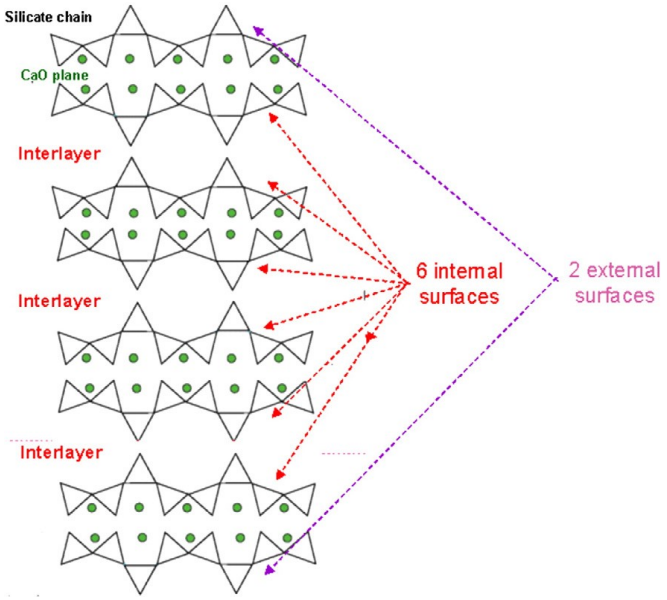

Figure 5-2: Schematic representation of the structure of a C-A-S-H particle (Bach, et al., 2013)

Of additional interest is the effect of the fraction of calcium in the source binder on the hardening of the mix (Phair & van Deventer, 2001). It was generally observed that setting time had considerably decreased with an increase in slag content. This explains the large differences in compressive strength observed between K-based and Na-based alkali activated binders for the 100% slag mixtures compared to the 50% fly ash-slag

mixtures. The addition of fly ash somewhat retards the setting time and decreases the viscosity of the mix, allowing the sodium activators to perform generally better than the mixtures with no fly ash.

The early-age response of the fly ash-slag blends is more favorable for the Na-based alkali activated binders. This can be attributed to the highly exothermic response of the sodium hydroxide dissociation compared to that of potassium with the addition of water to the mix. Na^+ is known to have a higher charge density (Z/r) and more exothermic hydration energy than K^+ (Fernández-Jiménez, et al., 2013). This initial release of heat accelerates the polymerization process of the binder resulting in the high early age strengths being observed for the fly ash-slag blends (fly ash requires activation energy in the form of heat for the reaction to occur). These trends are more prominent in the isothermal calorimetric signatures of these systems shown in the following section.

Analyzing the compressive strengths in terms of the silica modulus (M_s) also reveals a general trend. It has been found that samples activated using lower M_s ratios (ranging between 1.0-1.5) exhibit higher compressive strengths. This is because at high M_s ratios, there are not enough OH^- ions present in solution to adequately stabilize the solution and polymerization proceeds fairly quickly leading to high viscosity values with dissolutions rates also expected to be lower. A lower M_s ratio is expected to increase nucleation and crystal growth, which will provide for the expulsion of water from the newly formed structure leading to an initial decrease in viscosity. However if the M_s ratio is too low, the increased solid content of the paste starts to become a destabilizing factor while most added Na or K ions cannot be accommodated in the final structure (van Jaarsveld & van Deventer, 1999).

5.2 Isothermal Calorimetric Studies on Slag Mortars

Figure 5-3 shows the heat evolution curves of 100% slag pastes proportioned using an n value of 0.05 and M_s values of 1, 1.5 and 2. The experiments were carried out at 25°C. The calorimetric response exhibits two main peaks. The very narrow peak that occurs within the first two hours of mixing generally corresponds to the particle wetting and the dissolution of the slag and fly ash particles (Shi & Day, 1995; Ravikumar & Neithalath, 2012). However, in these particular mixtures, the dissolution peaks are most likely masked by the heat generated during the alkali activator dissociation. Of interest is that the dormant period, which is typical in the hydration of ordinary portland cement pastes, is absent in the Na-based systems. Rather it appears the acceleration peak that usually follows the dormant period is superimposed on the downward slope of the dissolution peaks. The further verifies the effects of the hydration energy of Na^+ cations, which accelerates the polycondensation of the gel structure and initiates the diffusion controlled stage within the first few hours of mixing. This proves to be favorable for Na-based fly ash-slag blends with lower viscosities than those of 100% slag mortars during early-ages (as evident in Figure 5-1a); however the lack of the dormant period does not allow for proper network organization of the resultant binder which results in the lower later-age strengths when compared to the K-based binders.

The shape of the calorimetric signatures of the K-based binders is very similar to that of OPC hydration even though the significant features are different with respect to their magnitudes and their occurrences in the time scale. The induction period of the potassium activated slag samples are considerably longer than that of OPC pastes. This is due to the time required for the ionic species in solution to reach a critical concentration

before depositing reaction products on the particle surfaces (Chithiraputhiran & Neithalath, 2013).

An increase in M_s values (or a reduction in alkalinity) generally causes a reduction of the initial dissolution peak. It can be seen that the highest peak occurs for the samples activated with M_s parameters of 1 and 1.5, with the M_s of 2 being lower and shifted to the right, suggesting improved activation when lower M_s values are used. This trend is supported by the compressive strength data in Figure 5-1(a). Studies have found that when alkaline activation is insufficient and becomes the main factor slowing down the hydration of slag, a lower silica modulus is preferred, with the optimum moduli for basic slag lying between 1.0-1.5 (Wang, et al., 1994).

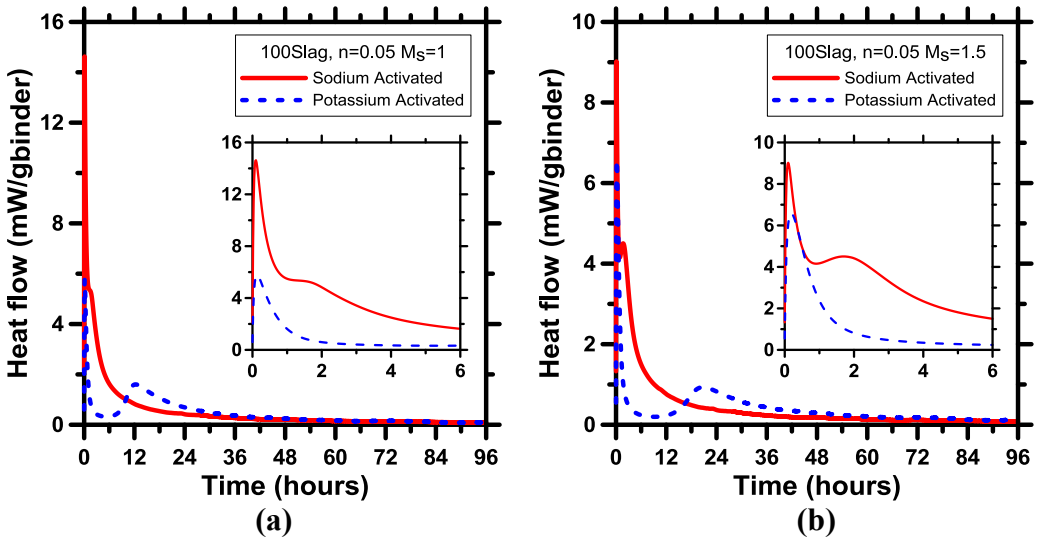

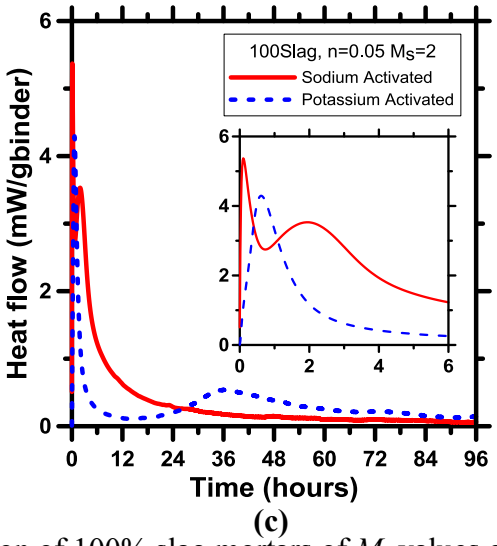

Figure 5-3: Heat evolution of 100% slag mortars of M_s values of (a) 1, (b) 1.5 and (c) 2.

Figure 5-4 shows the cumulative heat flow after 96h of reaction for the slag mixtures activated using potassium silicate and sodium silicate powders. The initial rising portion depicts the heat release contribution due to alkali dissociation along with the wetting and dissolution of the slag particles. The induction period of the K-based mortars is represented by the relatively flatter region in the cumulative heat release curve between the initial dissolution rise and the second acceleration rise. This pronounced plateau is absent for the Na-based mortars, as they do not have any distinct dormant period (Chithiraputhiran & Neithalath, 2013; Ravikumar & Neithalath, 2012). The general trend of the curves show the higher the alkalinity of the mortar (i.e. lower M_s values at the same n value), the higher the total cumulative heat release. This is because a higher alkalinity facilitates enhanced dissolution of slag particles and also the reaction of binder material after the dormant period, as can be observed from the larger acceleration peaks for the lower M_s mortars in Figure 5-3 (Chithiraputhiran & Neithalath, 2013; Chithiraputhiran, 2012).

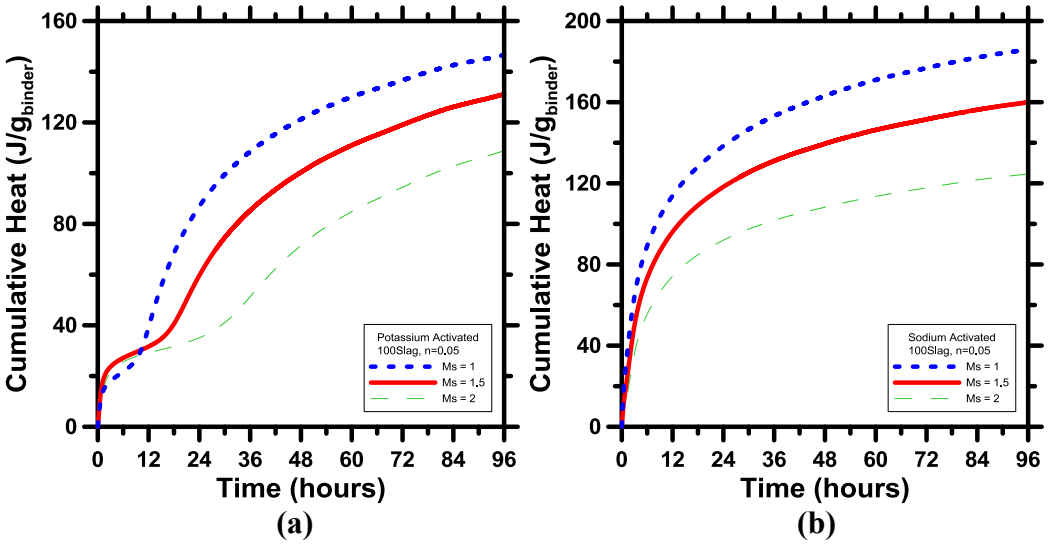

Figure 5-4: Cumulative heat release response for 100% slag mortars activated with (a) potassium silicate and (b) sodium silicate

5.3 Isothermal Calorimetric Studies on Fly ash-Slag Blend Mortars

Figure 5-5 shows the heat evolution curves of the 50% fly ash-slag blends using an n value of 0.05 and M_s values of 1, 1.5 and 2. The behavior of the blended Na-based systems are somewhat similar to those of the 100% slag mortars, in that the calorimetric response still lack a visible dormant period with the initial dissolution peak being combined with the acceleration peak. The cumulative heat flow shown in Figure 5-5b also follows the same trends as Figure 5-4 with the lower alkalinity mortars depicting a higher total cumulative heat release, and thus enhanced reaction.

The response of the potassium activated systems are also similar in nature to that of the 100% slag blends, with the heat generated during dissolution increasing with a reduction in the M_s value, along with the acceleration peak occurring earlier and steeper with reducing M_s. This is because the increase in OH^- ions due to the increase in alkali hydroxide content to reach the same n value result in increased source material

dissolution (breaking of T-O bonds faster, where T is Si, Al or Ca) (Altan & Erdoğan, 2012). This allows the ionic species in solution to reach the critical concentration to form reaction products earlier, as indicated by the acceleration peaks. In addition, the acceleration peak is higher for samples with lower M_s values, indicating the increased extent of the reaction (Altan & Erdoğan, 2012).

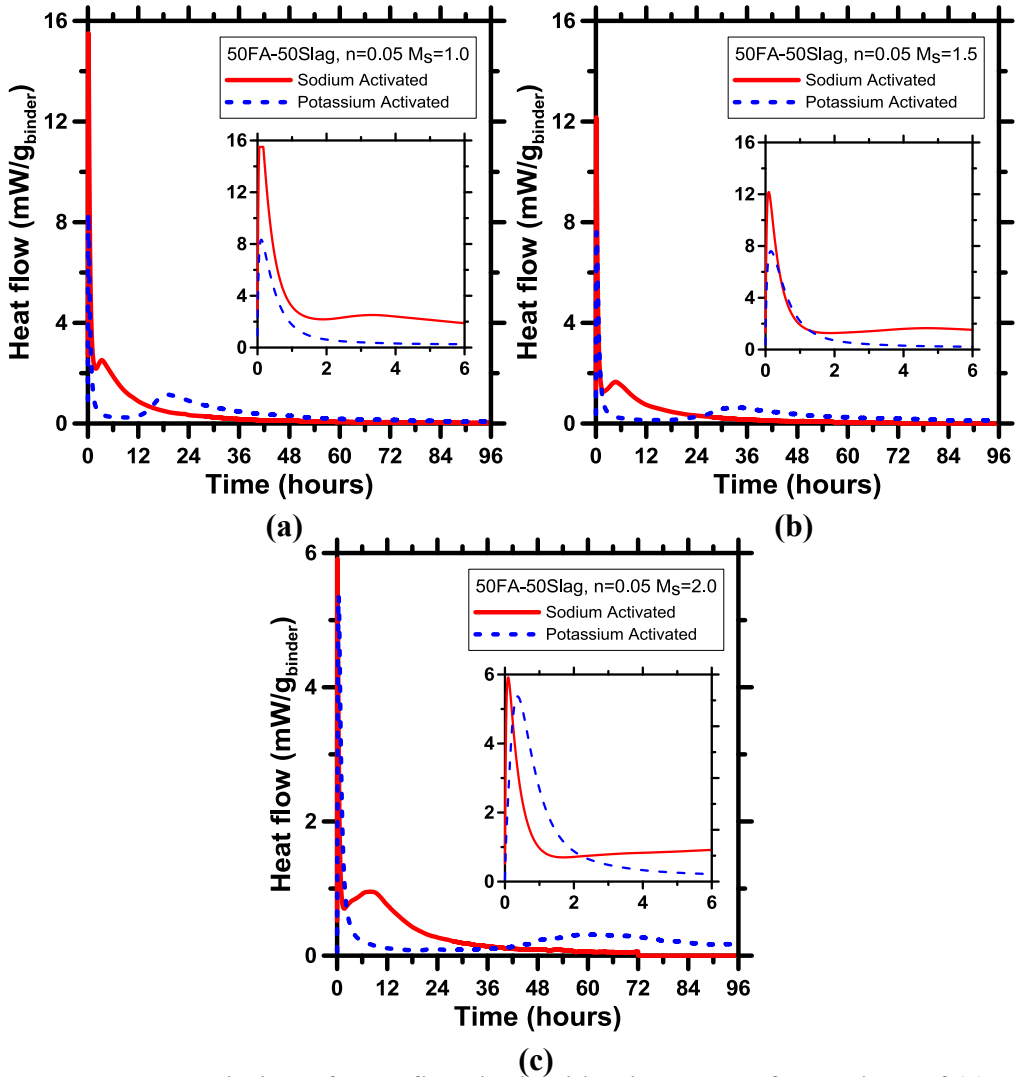

Figure 5-5: Heat evolution of 50% fly ash-slag blend mortars of M_s values of (a) 1, (b) 1.5 and (c) 2

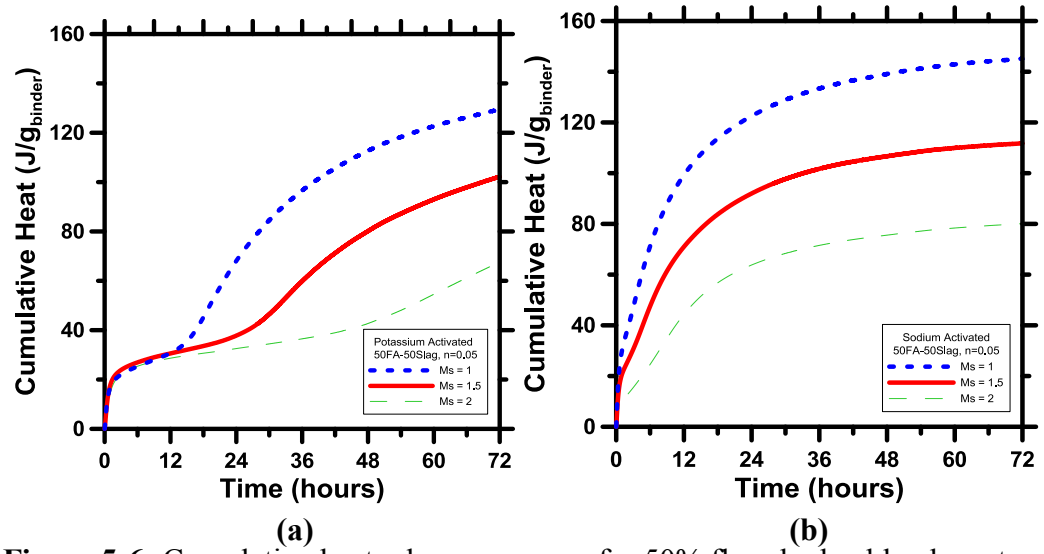

Figure 5-6: Cumulative heat release response for 50% fly ash-slag blend mortars activated with (a) potassium silicate and (b) sodium silicate

5.4 Effect of Leaching on the Electrical Solution Conductivity of the Mixes

The electrical conductivity of the alkali activated specimens were taken to capture the leaching effects of the unreacted ions (Na^+ or K^+, OH^- and Ca^{2+}) within the pore solutions of the specimens. Previous studies indicate that the conductivity contribution of the Ca^{2+} ions released is negligible, thus any increase of the conductivity of the distilled water will predominately be caused by the release Na^+/K^+ and OH^- ions into solution (Snyder, et al., 2003). A higher ion concentration within the pore solution is indicative of the binders' ability to continue the reaction process at later ages.

Figure 5-7 below shows the changes in electrical conductivity with time for the deionized water in which the alkali activated specimens (activated with an M_s of 1.5) were stored for several days. The initial increase in conductivity can be attributed to the leaching of the highly concentrated pore solution from the pore spaces of the specimens as the internal system attempts to attain equilibrium with the external environment

(leachate solution). However, as the ion concentration of the internal pore solution is reduced through this diffusion effect, it attempts to recover its original ion concentration by drawing out the loosely bound Na^+/K^+ and OH^- ions from the surrounding reaction product, which then is also leached out to maintain external equilibrium. This is represented by the linear region in the conductivity plots, signifying the gradual increase of the leachate solution conductivity with time after the initial jump.

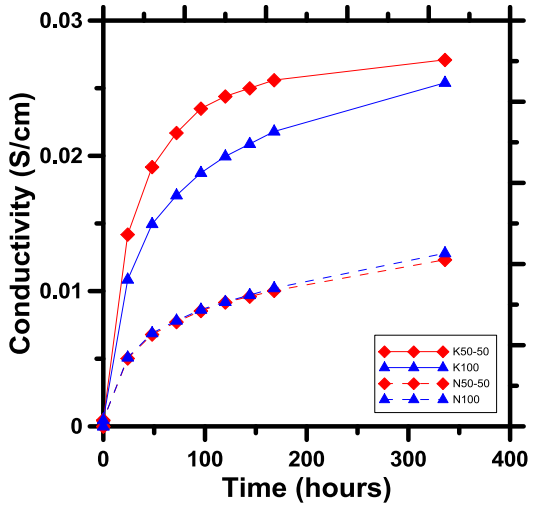

Figure 5-7: Electrical solution conductivity of mixes activated using an M_s of 1.5

Due to the assumption that the electrical conductivity of the pore solution is due to the contribution of the Na^+, K^+ and OH^- ions alone (Snyder, et al., 2003), it is reasonable to assume that the leachate solution is slowly turning into a weak KOH or NaOH (depending on the alkali activator) solution. This assumption allows the determination of the quantity of ions released into solution by comparing the conductivity of the leachate solution with the equivalent conductivity of the representative KOH or NaOH solution. Figure 5-8 shows the conductivity of KOH and NaOH solutions as a function of solution concentration (i.e. molarity of KOH/NaOH). It can be seen that at

any given concentration, the conductivities of the KOH and NaOH solutions are roughly the same. This can be attributed to the fact that regardless of the type of alkali solution, the OH^- concentration is the same for both, which is the most significant contributor to the pore solution conductivity; its equivalent conductivity (198 cm^2 S/mol) is a factor of two greater than that for sodium (50.1 cm^2 S/mol) and potassium (73.5 cm^2 S/mol) (Snyder, et al., 2003).

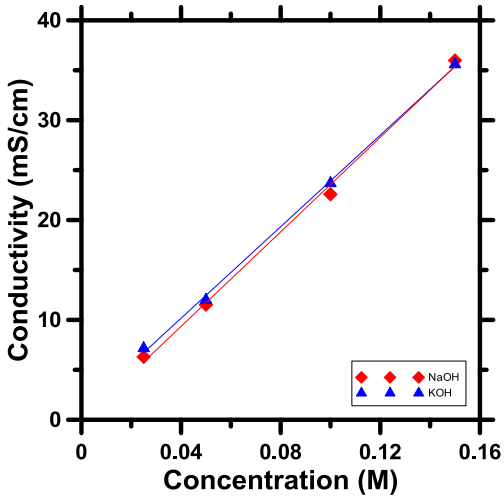

Figure 5-8: Conductivity of NaOH/KOH solutions as a function of molarity

Table 5-1 summarizes the initial and final concentrations of the leachate solutions represented as equivalent KOH or NaOH solutions, as determined from the conductivity-concentration relationship shown in Figure 5-7.

Table 5-1: Representative alkali hydroxide concentrations of leachate solutions

Alkali Activator	Binder composition	Initial Concentration	Final Concentration
Potassium	50% FA-Slag Blend	0.0576	0.1073
	100% Slag	0.043	0.0908
Sodium	50% FA-Slag Blend	0.0221	0.0529
	100% Slag	0.0224	0.054

It comes as no surprise that the potassium activated pastes exhibit higher leachate solution conductivities. This can again be linked back to K-based binders being able to retain free water and maintain lower viscosity at the time of mixing. With a more exothermic response of the sodium silicate powders dissociation, along with the Na^+ cation's larger solvated ion radius (Khale & Chaudhary, 2007; Phair & van Deventer, 2001; Provis & van Deventer, 2007), the pore space of the sodium activated binders would contain much less water that can be used to facilitate ion transportation, resulting in reduced amounts of leaching. This also explains why the later-age reaction process of the Na-based powder activated alkali activated binders is much slower than the K-based powder activated binders (as indicated by compressive strength development). Even though the water does not physically participate in the hydration process (unlike OPC pastes), water plays the role of a reaction medium that resides within the pores of the system and facilitates ion transportation during the reaction process (Duxson, et al., 2007), and thus requisite amounts of water is essential for the reaction process to continue.

5.5 Reaction Product in Powder Sodium Silicate Activated Slag and Fly ash – Slag Pastes

The previous sections have dealt with the analysis of the influence of the alkali activator on the compressive strength and isothermal heat flow response of activated slag and fly ash-slag mortars. Since the binders, alkali content and the composition of the activating agent influence the reaction product formation, a detailed analysis of the reaction products is attempted in this section with the use of Attenuated Total Reflectance – Fourier Transform Infrared (ATR-FTIR) Spectroscopy.

5.5.1. FTIR Analysis of activated slag pastes

It has been established that the alkali activation of slag results in the formation of a low Ca/Si ratio C-S-H and C-A-S-H gels as the principal reaction product (Wang & Scrivener, 1995; Yip & Lukey, 2005; Song, et al., 2000). The discussions in this section will be limited to the stretching vibrations of Si-O-Si units, as they can be used to represent the signature of the composition of the reaction products. In general the Si-O-Si stretching bands are observed at a wavenumber of 950-1000cm^{-1} (García-Lodeiro, et al., 2008; Bernal, et al., 2011; Palomo, et al., 2007). Figure 5-9 shows the FTIR spectra of the starting slag showing one main peak occurring at 928 cm^{-1} recognized as the Si-O stretching of the SiO_4 tetrahedra (Fernández-Jiménez, et al., 2003). In the alkali activated slag pastes, this band representing the asymmetric stretching vibrations of the Si-O-Si bands has been shifted to higher wavenumber values of 940-955 cm^{-1}. Figure 5-10 represents the 3 and 28 day FTIR spectra of the potassium silicate and sodium silicate activated slag pastes with M_s values of 1, 1.5 and 2. The observed shifts of the Si-O-Si

stretching bands can be attributed to the formation of a more condensed tetrahedral species (Chithiraputhiran, 2012). The FTIR spectra also contains bands of calcite (C-O) occurring at 1370-1420 cm^{-1} that occurs in the event of carbonation. The peaks detected between 3330-3375 cm^{-1} and 1630-1645 cm^{-1} represent stretching and bending modes of OH^- groups present in H_2O and the hydration products. The distinct peaks of calcium hydroxide (CH) that occur at ~3365 cm^{-1} in most OPC pastes is absent in the spectra of slag as CH cannot precipitate in these systems due to its higher solubility compared to C-S-H and C-A-S-H (Chithiraputhiran, 2012).

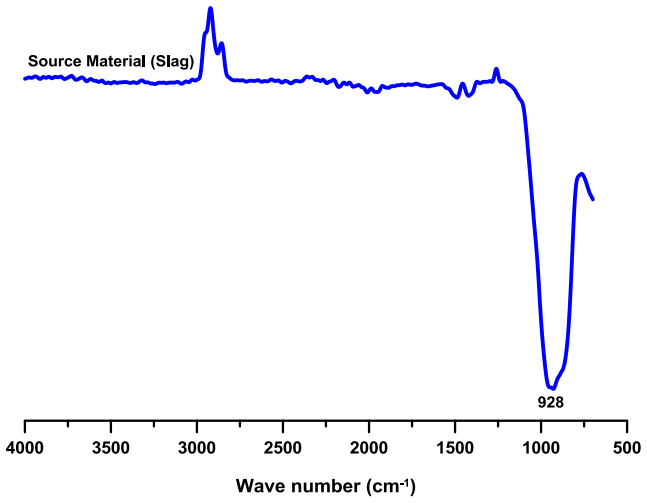

Figure 5-9: FTIR spectra of source slag (Chithiraputhiran, 2012)

A shift to a higher wavenumber generally indicates the effect of a high Si content within the C-S-H gel (or a lower Ca/Si ratio) (Palacios & Puertas, 2006). Thus, it is expected that the pastes activated using higher M_s values (in which case the content of SiO_2 is increased) shows characteristic signatures shifting towards higher wavenumbers, as shown in Figure 5-10. This trend is more pronounced with longer curing durations. The solubility of Si is known to increase with pH content of the paste, whereas that of Ca

decreases. Hence, the systems activated with high silica concentrations, i.e. higher M_s values, tend to produce C-S-H gels with a lower Ca/Si ratio. This results in the production of a Q^3 silicon that has the ability to cross-link between adjacent silicon chains (Fernández-Jiménez, et al., 2003). This is in contrast with the C-S-H gels produced in OPC pastes which predominantly contain Q^1 and Q^2 units (Schneider, et al., 2001). The 'Q^n notation' is often adopted for describing building units of silicon, where Q stands for a silicon atom and the superscript *n* indicates the connectivity, i.e. the number of bridging oxygens (–OSi) surrounding the central silicon atom (Klinowski, et al., 1998). The IR absorption bands witnessed in the range of 940-960 cm^{-1} in Figure 5-10 is consistent with the predominance of Q^2 and Q^3 silicates (Dimas, et al., 2009).

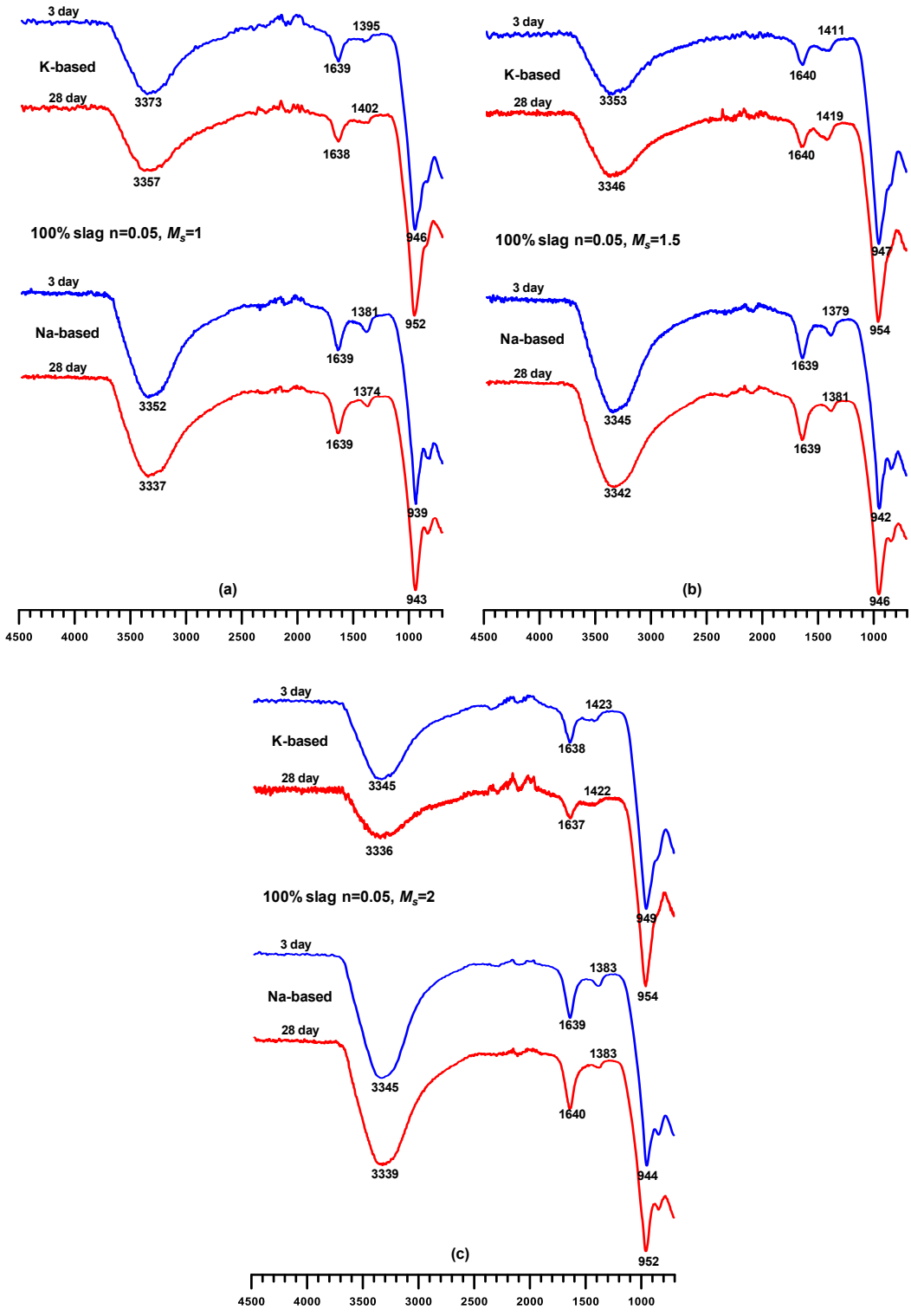

Figure 5-10: ATR-FTIR spectroscopy of 100% slag binders activated with n=0.05and M_s values of (a) 1, (b) 1.5 and (c) 2

5.5.2. FTIR analysis of activated fly ash-slag pastes

Figure 5-11 shows the ATR-FTIR analysis of the 50% fly ash-slag blends. The same activation parameters (*n* of 0.05 and M_s of 1, 1.5 and 2) were used to prepare these activated blends. The principle Si-O stretching bands of these pastes occur within the 950-965 cm^{-1} range. The high wavenumber of these mixtures is attributed to the reaction product having Ca/Si ratios that are much lower to that of the activated slag pastes (Chithiraputhiran, 2012). The alkaline activation of fly ash leads to the formation of alkaline aluminosilicates, i.e., K-A-S-H in K-based systems and N-A-S-H in Na-based systems. These gel structures are of an amorphous nature with a 3D network akin to a zeolitic gel structure. As shown previously in Chapter 4 of this document, the FTIR spectrum of the alkaline aluminosilicate generally has a band associated to Si-O-Si stretching vibrations at 990-1010 cm^{-1} (Puertas, et al., 2000), however these higher wavenumbers are not detected in the IR spectra of the fly ash-slag blends. This indicates the influence of the calcium bearing slag in the reaction product formation (Chithiraputhiran, 2012). The effects of the silica modulus exhibit similar trends as those for the activated 100% slag pastes, with an increase in wavenumber with an increase in M_s value of the activator. In addition, stretching and bending modes of OH^- groups of H_2O and the reaction products were also observed at 3330-3365 cm^{-1} and at 1630-1645 cm^{-1} as was in the slag pastes.

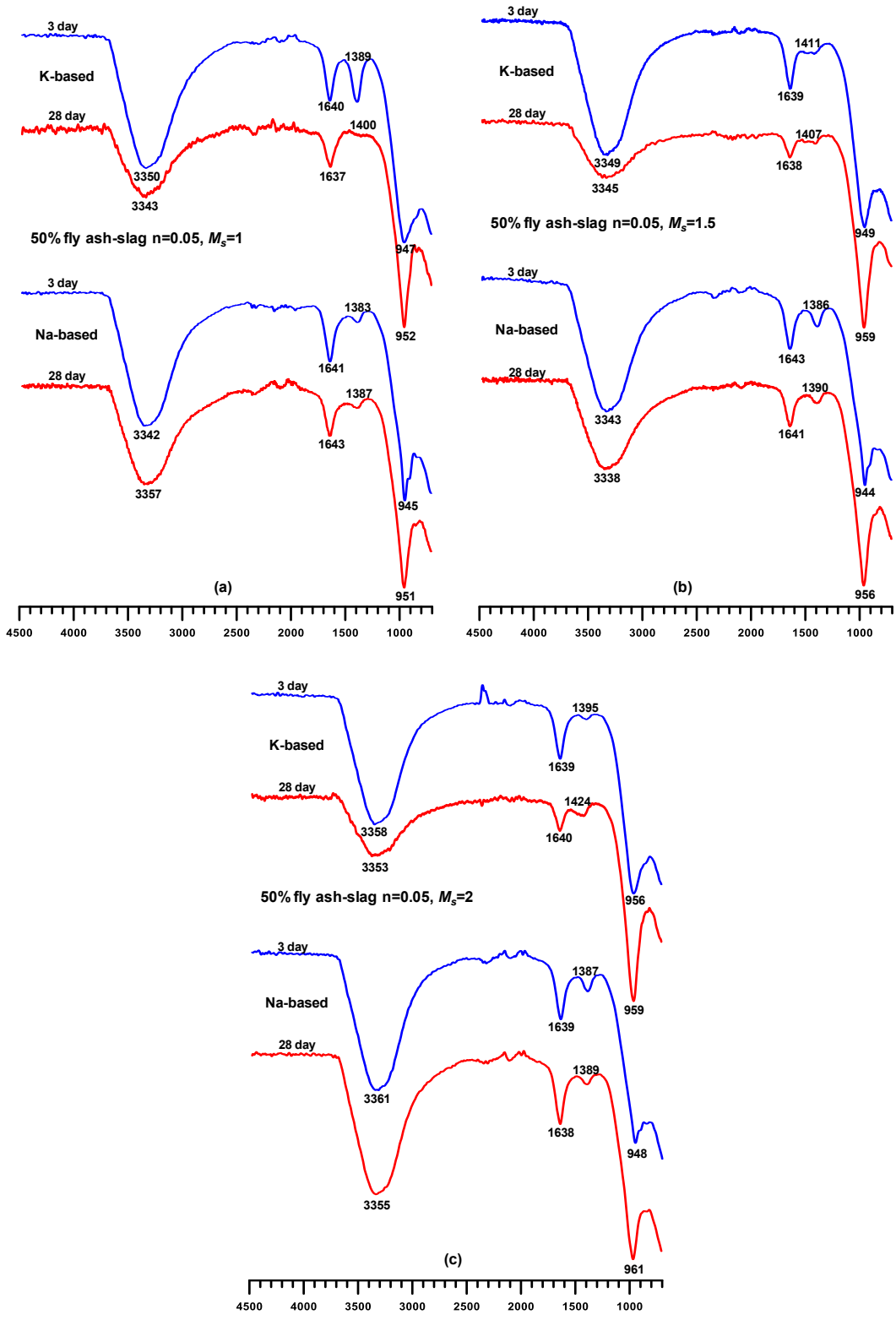

Figure 5-11: ATR-FTIR spectroscopy of 50% fly ash-slag binders activated with n=0.05and M_s values of (a) 1, (b) 1.5 and (c) 2

5.5.3. Effect of alkali cation on reaction products

The peaks associated with the vibrations of the asymmetric Si-O-Si tetrahedral (between 940-965 cm^{-1}) are generally indicative of the degree of polymerization (van Jaarsveld & van Deventer, 1999), with higher wavenumbers being linked with higher degrees of polymerization. The values obtained are fairly similar although there seems to generally be a shift to higher wavenumbers in the case of the K-based binders. For these binders, the higher frequencies of the asymmetric vibrations of the Si-O-Si bonds could signify an increased degree of polycondensation due to the presence of potassium (van Jaarsveld & van Deventer, 1999). This also supports the compressive strength results discussed in earlier sections.

It is also interesting to note that for any given mixture with constant binder composition and activator used, the peaks between 940-965 cm^{-1} seem to generally shift towards lower wavenumbers as the M_s ratios are decreased. The reason for this is an increasing number of Al substituting for Si as both the alkalinity and number of charge balancing ions increase (van Jaarsveld & van Deventer, 1999).

5.6 Porosity of Powder Activated Slag and Fly ash-Slag Pastes using Vacuum Saturation Method

The results in Table 5-2 show the amount of water absorption of the alkali activated mixes with an M_s ratio of 1.5 using the vacuum saturation method described in previous sections. The variation in the water absorption (which can be related to the porosity of the sample) are generally in good agreement with the mechanical strength

development observed in the mortars, with the potassium activated mixes showing both more strength development and reduced porosity after 14 days of curing.

Table 5-2: Absorption of alkali activated mortars using Vacuum Saturation Method

Alkali Activator	Binder composition	Water Absorption (wt.%)
Potassium	50% FA-Slag Blend	12.36
	100% Slag	11.4
Sodium	50% FA-Slag Blend	14.09
	100% Slag	12.8

It can be seen that the higher content of slag leads to significantly lower water absorption, which is coherent with a reduced porosity and a refined pore structure. These trends are in agreement with previous studies (Ravikumar, 2012) where the porosities of alkali activated concretes using slag were found to be lower than those made using fly ash. However, the increased water absorption of the K-based 50% fly ash-slag blend mortars can tentatively also be attributed to thermal cracking induced during the drying process at 105°C, as shown in Figure 5-12.

Figure 5-12: Photo of the Vacuum Saturation test samples after removal from the oven at 105°C for 24 h

5.7 Summary

The influence of the alkali cation used in the alkali activation of slag and fly ash-slag blends using powder silicates are discussed in this chapter. It was found that mixtures activated using potassium are more effective in producing binders with favorable mechanical properties. Isothermal calorimetric tests showed a high release of heat for Na-based binders which accelerate the polycondensation process of Na-based binders, initiating the diffusion process much earlier compared to K-based binders. Electrical conductivity measurements reveal that the alkali hydroxide concentrations of the leachate solutions were higher for K-based binders, indicating a more alkali saturated pore solution that allows the reaction process to continue at later ages. The trends of the porosity of the samples established using vacuum saturation methods are generally in good agreement with the mechanical strength development observed in the mortars, with the potassium activated mixes showing reduced porosity after 14 days of curing.

Chapter 6

CONCLUSION

6.1. Influence of Thermal Curing on Strength and Reaction Products of NaOH and Sodium Silicate Activated Fly Ash

The chief conclusions drawn in the study of thermal curing on the strength and reaction products of NaOH and sodium silicate activated fly ash were as follows:

- For waterglass based mixtures the samples activated under sealed conditions generally exhibit higher strengths. Unsealed specimens generally resulted in lower compressive strengths, possibly due to carbonation and the reduction in the availability of free water for the reaction to continue.
- At higher n and M_s ratios the curing conditions do not affect samples greatly as they contain high amounts of reactive ions and soluble silica to obtain favorable compressive strengths, thereby minimizing the influence of water retained during the curing process. However, the consequence of these high n and M_s values are the excessive amounts of leaching that cause dimensional instability.
- For NaOH based mixtures, the strengths are generally independent of whether the samples were cured in sealed or unsealed conditions. This can possibly be explained by the Al dissolving more readily than Si when carbonation occurs, which causes greater precipitation of the Al rich sodium aluminosilicate hydrate (N-A-S-H) gel. In other words, carbonation does not adversely influence the strength of NaOH activated fly ash mixtures.

- When microwave curing is used, the compressive strength attained after 45 min of microwaving curing surpasses the compressive strength of unsealed heat cured samples after 48 h activated with the same parameters.
- Where microwave curing is used, until 60-90 min of microwave curing at 360 W, increased curing times result in increased strengths; after which strength decreases. This can be attributed to the complete evaporation of all free water within the specimen. Excess of microwave heating beyond this point results in decay of the sample microstructure.
- Sealing the samples during microwave radiation traps the water in the system, preventing evaporation of free water. However, this in turn traps heat since heating of the sample is primarily due to the heating of the pore solution, causing moisture loss to occur much faster.
- When combined thermal and microwave curing is utilized, there is no appreciable strength gain after 60 min of microwave curing. Instead, the excessive temperatures after microwave curing for prolonged periods have a tendency to decay the microstructure and reduce mechanical strength.
- TGA studies confirm that there is very little free water remaining in the system for samples that undergo a microwave curing regime.
- From the FTIR results, the wavenumbers produced from binders activated using only NaOH are not as high as those activated using waterglass. This indicates that the degree of silica polymerization is not as high and the gel formed is the intermediate, aluminum-rich phase.

- FTIR results also reveal that gel polymerization of the microwaved samples cured at 240 W does result in a higher polymerization of the gel structure (with wavenumbers reaching as high as 1001 cm^{-1}). This proves the potential for the effectiveness of microwave curing over conventional heat curing if the excessive temperatures that cause microcracking of the sample microstructure can be controlled.

6.2. Effect of Activator Characteristics on the Reaction Product Formation in Fly ash/Slag Binders Activated Using Alkali Silicate Powders and Hydroxides

The main conclusions drawn in the study of the effect of activator characteristics on the reaction product formation in fly ash/slag binders activated using alkali silicate powders and hydroxides were as follows:

- The results of this study indicate that the binders activated using potassium based activators perform better than those activated using sodium based activators at later ages. This can be attributed to a number of reasons, namely the viscosity of the pastes, heat generated by the dissociation of the alkali activating powders into solution and the dissolution capabilities of the alkali activators. This can also be related to the fact that Na-based activating solutions and the resulting pastes are much more viscous and polymerize much faster, thus inhibiting the ability to perform proper mixing procedures.
- The early-age response of the fly ash-slag blends is more favorable when Na-based activators are used. This can be attributed to highly exothermic response of the sodium hydroxide dissociation compared to that of potassium with the addition of water to the mix.

- It has been found that samples activated using lower M_s ratios (ranging between 1.0-1.5) exhibit higher compressive strengths. This is because at high M_s ratios, there are not sufficient OH^- ions present in solution to adequately stabilize the solution and polymerization proceeds fairly quickly leading to high viscosity values with dissolutions rates also expected to be lower.
- Isothermal calorimetric studies reveal a lack of the typical dormant period of mixes activated using sodium silicates. Rather it appears the acceleration peak that usually follows the dormant period is superimposed on the downward slope of the dissolution peaks. This does not allow for proper network organization of the resultant binder which results in the lower later-age strengths when compared to the K-based binders.
- Electrical solution conductivity measurements reveal that the potassium activated pastes exhibit the higher leachate solution conductivities. This can again be linked back to K-based binders being able to retain free water and maintain lower viscosity at the time of mixing.
- FTIR spectroscopic analysis of the hydrated pastes shows the effects of the silica modulus, with an increase in wavenumber observed for an increase in M_s value of the activator. This is because an increasing number of Al substitutes for Si as both the alkalinity and number of charge balancing ions increase.
- The wavenumber values obtained are fairly similar for both binders; however there seems to be a general shift to higher wavenumbers in the case of the K-based binders. For these binders, the higher frequencies of the asymmetric

vibrations of the Si-O-Si bonds could signify an increased degree of polycondensation due to the presence of potassium.

- The trends of the porosity of the samples established using vacuum saturation are generally in good agreement with the mechanical strength development observed in the mortars, with the potassium activated mixes showing reduced porosity after 14 days of curing.

REFERENCES

Alonso, S. & Palomo, A., 2001. Alkaline activation of metakaolin and calcium hydroxide mixtures: influence of temperature, activator concentration and solids ratio. *Materials Letters,* January, 47(1–2), pp. 55-62.

Altan, E. & Erdoğan, S. T., 2012. Alkali activation of a slag at ambient and elevated temperatures. *Cement and Concrete Composites,* 34(2), pp. 131-139.

Astutiningsih, S. & Liu, Y., 2005. Geopolymerisation of Australian slag with effective dissolution by the alkali. In: *Geopolymer, Green Chemistry and Sustainable Development Solutions: Proceedings of the World Congress Geopolymer 2005*. Saint Quentin: Geopolymer Institute, pp. 69-73.

Bach, T. et al., 2013. Retention of alkali ions by hydrated low-pH cements: Mechanism and Na+/K+ selectivity. *Cement and Concrete Research,* Volume 51, pp. 14-21.

Bakharev, T., 2006. Thermal behaviour of geopolymers prepared using class F fly ash and elevated temperature curing. *Cement and Concrete Research,* 36(6), pp. 1134-1147.

Bentz, D. P. et al., 1994. Cellular automaton simulations of cement hydration and microstructure development. *Modelling and Simulation in Materials Science and Engineering,* 1 July, 2(4), p. 783.

Bernal, S. A. et al., 2011. Effect of binder content on the performance of alkali-activated slag concretes. *Cement and Concrete Research,* January, 41(1), pp. 1-8.

Büyüköztürk, O., Yu, T.-Y. & Ortega, J. A., 2006. A methodology for determining complex permittivity of construction materials based on transmission-only coherent, wide-bandwidth free-space measurements. *Cement and Concrete Composites,* 28(4), pp. 349-359.

Cha-um, W., Rattanadecho, P. & Pakdee, W., 2009. Experimental analysis of microwave heating of dielectric materials using a rectangular wave guide (MODE: TE10) (Case study: Water layer and saturated porous medium). *Experimental Thermal and Fluid Science,* 33(3), pp. 472-481.

Chi, M. & Huang, R., 2013. Binding mechanism and properties of alkali-activated fly ash/slag mortars. *Construction and Building Materials,* Volume 40, pp. 291-298.

Chithiraputhiran, S. & Neithalath, N., 2013. Isothermal reaction kinetics and temperature dependence of alkali activation of slag, fly ash and their blends. *Construction and Building Materials,* August, Volume 45, pp. 233-242.

Chithiraputhiran, S. R., 2012. *Kinetics of Alkaline Activation of Slag and Fly ash-Slag Systems,* Tempe: s.n.

Choate, W. T., 2003. *Energy and Emission Reduction Opportunities for the Cement Industry,* Columbia, MD: s.n.

Clark, D. E., Folz, D. C. & West, J. K., 2000. Processing materials with microwave energy. *Materials Science and Engineering: A,* 287(2), pp. 153-158.

Criado, M., Fernández-Jiménez, A. & Palomo, A., 2010. Alkali activation of fly ash: Effect of curing conditions on reaction and - Part III. *Fuel,* Issue 89, p. 3185–3192.

Criado, M., Palomo, A. & Fernández Jiménez, A., 2005. Alkali activation of fly ash Part I - Effect of curing conditions on the carbonation of the reaction products. *Fuel,* Issue 84, p. 2048–2054.

Davidovits, J., 1999. *Chemistry of Geopolymeric Systems, Terminology.* Saint-Quentin, France, s.n., pp. 9-22.

Davidovits, J., 2005. Geopolymer chemistry and sustainable development. The Poly(sialate) terminology: a very useful and simple model for the promotion and understanding of green-chemistry. In: *Geopolymer, Green Chemistry and Sustainable Development Solutions: Proceedings of the World Congress Geopolymer.* Saint Quentin: Geopolymer Institute, pp. 69-73.

Dimas, D., Giannopoulou, J. & Panias, D., 2009. Polymerization in sodium silicate solutions: a fundamental process in geopolymerization technology. *Journal of Materials Science,* 1 July, 44(14), pp. 3719-3730.

Duxson, P. et al., 2007. Geopolymer technology: the current state of the art. *Journal of Materials Science,* 1 May, 42(9), pp. 2917-2933.

Duxson, P., Lukey, G., Separovic, F. & van Deventer, J., 2005. Effect of Alkali Cations on Aluminum Incorporation in Geopolymeric Gels. *Industrial & Engineering Chemistry Research,* 1 February, 44(4), pp. 832-839.

Fernández-Jiménez, A., Palomo, A. & Criado, M., 2005. Microstructure development of alkali-activated fly ash cement: a descriptive model. *Cement and Concrete Research,* June, 35(6), pp. 1204-1209.

Fernández-Jiménez, A., Palomo, A., Sobrados, I. & Sanz, J., 2006. The role played by the reactive alumina content in the alkaline activation of fly ashes. *Microporous and Mesoporous Materials,* 15 April, 91(1–3), pp. 111-119.

Fernández-Jiménez, A. & Puertas, F., 2001. Setting of alkali-activated slag cement. Influence of activator nature. *Advances in Cement Research,* 7 January, 13(3), pp. 115-121.

Fernández-Jiménez, A., Puertas, F., Sobrados, I. & Sanz, J., 2003. Structure of Calcium Silicate Hydrates Formed in Alkaline-Activated Slag: Influence of the Type of Alkaline Activator. *Journal of the American Ceramic Society,* 96(8), p. 1389–1394.

Fernández-Jiménez, A. et al., 2013. "Metakaolin-Slag-Clinker Blends." The Role of Na+ or K+ as Alkaline Activators of Theses Ternary Blends. *Journal of the American Ceramic Society,* 96(6), p. 1991–1998.

García-Lodeiro, I., Fernández-Jiménez, A., Blanco, M. T. & Palomo, A., 2008. FTIR study of the sol–gel synthesis of cementitious gels: C–S–H and N–A–S–H. *Journal of Sol-Gel Science and Technology,* 1 January, 45(1), pp. 63-72.

Glukhovsky, V., 1959. *Soil silicates.* Kiev: Gosstroi Publishers.

Glukhovsky, V., 1965. *Soil silicates, Their Properties, Technology and Manufacturing and Fields of Application.* Kiev: Doct Tech Sc. Degree thesis. Civil Engineering Institute.

Glukhovsky, V., 1994. *Ancient, modern and future concretes.* Kiev, Ukraine, s.n., pp. 1-8.

Gubb, T. et al., 2011. *Microwave Enhanced Drying and Firing of Geopolymers.* Daytona Beach, Florida, s.n.

Gubb, T. et al., 2011. *Microwave Processing of Geopolymers and Evolved Glass-Ceramic Composites Presentation.* Daytona Beach, Florida, 35th International Conference and Exposition on Advanced Ceramics and Composites.

Hajimohammadi, A., Provis, J. L. & van Deventer, J. S., 2011. The effect of silica availability on the mechanism of geopolymerisation. *Cement and Concrete Research,* March, 41(3), pp. 210-216.

Hardjito , D. & Rangan, B. V., 2005. *Develoment and properties of low-calcium fly ash-based geopolymer concrete,* Perth, Australia: s.n.

Hermann, E. et al., 1999. *Proceedings of Geopolymers.* s.l.:s.n.

Iowa State University of Science and Technology, n.d. *Laboratory 10: Thermogravimetric Analysis.* [Online] Available at: https://sites.google.com/a/iastate.edu/laboratory-10-thermogravimetric-analysis/history

Khale, D. & Chaudhary, R., 2007. Mechanism of geopolymerization and factors influencing its development: a review. *Journal of Materials Science,* 1 February, 42(3), pp. 729-746.

Klinowski, J. et al., 1998. Structural studies of tabasheer, an opal of plant origin. *PHILOSOPHICAL MAGAZINE A,,* 77(1), pp. 201-216.

Komnitsas, K., Zaharaki, D. & Perdikatsis, V., 2009. Effect of synthesis parameters on the compressive strength of low-calcium ferronickel slag inorganic polymers. *Journal of Hazardous Materials,* 161(2-3), pp. 760-768.

Kovalchuk, G., Fernández-Jiménez, A. & Palomo, A., 2007. Alkali activation of fly ash: Effect of thermal curing conditions on mechanical and microstructural development - Part II. *Fuel,* Issue 86, pp. 315-322.

Krivenko, P., 1994. *Alkaline Cements.* Kiev, Ukraine, s.n.

Lemougna, P. N., MacKenzie, K. J. & Melo, U. C., 2011. Synthesis and thermal properties of inorganic polymers (geopolymers) for structural and refractory applications from volcanic ash. *Ceramics International,* 37(8), pp. 3011-3018.

Li, C., Sun, H. & Li, L., 2010. A review: The comparison between alkali-activated slag (Si + Ca) and metakaolin (Si + Al) cements. *Cement and Concrete Research,* September, 40(9), pp. 1341-1349.

Li, D. et al., 2000. Study of properties on fly ash–slag complex cement. *Cement and Concrete Research,* 30(9), pp. 1381-1387.

Lizcano, M., Kim, H. S., Basu, S. & Radovic, M., 2012. Mechanical properties of sodium and potassium activated metakaolin-based geopolymers. *Journal of Materials Science,* 01 03, 47(6), pp. 2607-2616.

Mahasenan, N., Smith, S. & Humphreys, K., 2003. The Cement Industry and Global Climate Change: Current and Potential Future Cement Industry CO2 Emissions. In: J. Gale & Y. Kaya, eds. *Greenhouse Gas Control Technologies - 6th International Conference.* Oxford: Pergamon, pp. 995-1000.

Ma, Y., Hu, J. & Ye, G., 2012. The effect of activating solution on the mechanical strength, reaction rate, mineralogy, and microstructure of alkali-activated fly ash. *Journal of Materials Science,* June, 47(11), pp. 4568-4578.

McDonald, M. & Thompson, J. L., n.d. Sodium Silicate: A Binder for the 21st Centur. *Industrial Chemical Division.*

McDonald, M. & Thompson, J. L., n.d. *Sodium Silicate: A Binder for the 21st Century,* s.l.: The PQ Corporation.

Nelson, E. B., 1990. *Well Cementing.* Sugar Land(Texas): Schlumberger Educational Services.

Ortego, J. D., Barroeta, Y., Cartledge, F. K. & Akhter, H., 1991. Leaching effects on silicate polymerization. An FTIR and silicon-29 NMR study of lead and zinc in portland cement. *Environmental Science & Technology,* 25(6), pp. 1171-1174.

Palacios, M. & Puertas, F., 2006. Effect of Carbonation on Alkali-Activated Slag Paste. *Journal of the American Ceramic Society,* 89(10), p. 3211–3221.

Palomo, A. et al., 2007. Opc-fly ash cementitious systems: study of gel binders produced during alkaline hydration. *Journal of Materials Science,* 42(9), pp. 2958-2966.

Palomo, A. et al., 2005. hydration, Opc-fly ash cementitious systems: study of gel binders produced during alkaline. *Journal of Materials Science,* 1 May, 42(9), pp. 2958-2966.

PCA, 2003. Fly Ash, Slag, Silica Fume, and Natural Pozzolans. In: *Design and Control of Concrete Mixtures.* 14th ed. s.l.:Portland CementAssociation, pp. 57-72.

PerkinElmer, 2010. *Thermogravimetric Analysis (TGA): A Beginners Guide,* Waltham, MA: PerkinElmer, Inc..

Petermann, J., Saeed, A. & Hammons, M., 2010. Alkali-Activated Geopolymers: A Literature Review. *Materials and Manufacturing Directorate,* July.

Phair, J. & van Deventer, J., 2001. Effect of silicate activator pH on the leaching and material characteristics of waste-based inorganic polymers. *Minerals Engineering,* March, 14(3), pp. 289-304.

Provis, J. L. & van Deventer, J. S., 2007. Geopolymerisation kinetics. 1. In situ energy-dispersive X-ray diffractometry. *Chemical Engineering Science,* May, 62(9), pp. 2309-2317.

Puertas, F. & Fernández-Jiménez, A., 2003. Mineralogical and microstructural characterisation of alkali-activated fly ash/slag pastes. *Cement and Concrete Composites,* 25(3), pp. 287-292.

Puertas, F., Fernández-Jiménez, A. & Blanco-Varela, M., 2004. Pore solution in alkali-activated slag cement pastes. Relation to the composition and structure of calcium silicate hydrate. *Cement and Concrete Research,* January, 34(1), pp. 139-148.

Puertas, F., Martínez-Ramírez, S., Alonso, S. & Vázquez, T., 2000. Alkali-activated fly ash/slag cements: Strength behaviour and hydration products. *Cement and Concrete Research,* October, 30(10), pp. 1625-1632.

Purdon, A., 1940. The Action of Alkalis on blast-furnace slag. *Journal of the Society of Chemical Industry,* Volume 59, pp. 191-202.

Rahier, H., Simons, W., Mele, B. V. & Biesemans, M., 1997. Low-temperature synthesized aluminosilicate glasses: Part III Influence of the composition of the silicate solution on production, structure and properties. *Journal of Materials Science,* 1 May, 32(9), pp. 2237-2247.

Rangan, B. V., 2008. *Fly Ash-Based Geopolymer Concrete.* [Online] Available at: http://www.yourbuilding.org/Article/NewsDetail.aspx?p=83&id=1570

Ravikumar, D., 2012. *Property Development, Microstructure and Performance of Alkali Activated Fly Ash and Slag Systems,* Clarkson: ProQuest, UMI Dissertations Publishing 2012.

Ravikumar, D. & Neithalath, N., 2012. Effects of activator characteristics on the reaction product formation in slag binders activated using alkali silicate powder and NaOH. *Cement and Concrete Composites,* August, 34(7), pp. 809-818.

Ravikumar, D. & Neithalath, N., 2012. Reaction kinetics in sodium silicate powder and liquid activated slag binders evaluated using isothermal calorimetry. *Thermochimica Acta,* 20 October, Volume 546, pp. 32-43.

Ravikumar, D., Peethamparan, S. & Neithalath, N., 2010. Structure and strength of NaOH activated concretes containing fly ash or GGBFS as the sole binder. *Cement & Concrete Composites,* pp. 399-410.

RILEM TC, 1994. CPC 11.3 Absorption of water by concrete by immersion under vacuum. In: RILEM, ed. *RILEM Recommendations for the Testing and Use of Constructions Materials.* s.l.:E & FN SPON, pp. 36-37.

Roy, D. M., 1999. Alkali-activated cements Opportunities and challenges. *Cement and Concrete Research,* February, 29(2), pp. 249-254.

Schneider, J., Cincotto, M. & Panepucci, H., 2001. 29Si and 27Al high-resolution NMR characterization of calcium silicate hydrate phases in activated blast-furnace slag pastes. *Cement and Concrete Research,* July, 31(7), pp. 993-1001.

Shi, C. & Day, R., 1999. Early strength development and hydration of alkali-activated blast furnace slag/fly ash blends. *Advances in Cement Research,* 11(4), pp. 189-196.

Shi, C. & Day, R. L., 1995. A calorimetric study of early hydration of alkali-slag cements. *Cement and Concrete Research,* August, 25(6), pp. 1333-1346.

Shi, C. & Day, R. L., 1995. A calorimetric study of early hydration of alkali-slag cements. *Cement and Concrete Research,* August, 25(6), pp. 1333-1346.

Shulman, H. S., Fall, M. & Allan, S., 2007. *Microwave Assist Technology for Product Improvement and Energy Efficiency.* Jeju, South Korea, 4th Korea/Japan Symposium on Materials Science and Resources Recycling, pp. 142-46.

Skvara, F. D. J. S. P. K. L. P. S. M. D. K. B. M. M. L. S. R., n.d. *Concrete Based on Fly Ash Geopolymers,* Praha: s.n.

Škvára, F., Kopecký, L., Šmilauer, V. & Bittnar, Z., 2009. Material and structural characterization of alkali activated low-calcium brown coal fly ash. *Journal of Hazardous Materials,* 15 September, 168(2-3), pp. 711-720.

Smith, M. & Osborne, G., 1977. Slag/Fly Ash Cements. *World Cement Technology,* 8(6), pp. 223-224.

Snyder, K., Feng, X., Keen, B. & Mason, T., 2003. Estimating the electrical conductivity of cement paste pore solutions from OH−, K+ and Na+ concentrations. *Cement and Concrete Research,* June, 33(6), pp. 793-798.

Somaratna, J., Ravikumar, D. & Neithalath, N., 2010. Response of alkali activated fly ash mortars to microwave curing. *Cement and Concrete Research,* December, 40(12), pp. 1688-1696.

Song, S., Sohn, D., Jennings, H. & Mason, T., 2000. Hydration of alkali-activated ground granulated blast furnace slag. *Journal of Materials Science,* 1 January, 35(1), pp. 249-257.

Tuchbreiter, A. et al., 2001. High-throughput evaluation of olefin copolymer composition by means of attenuated total reflection Fourier tranform infrared spectroscopy. *Journal of combinatorial chemistry,* Nov-Dec, 3(6), pp. 598-603.

van Jaarsveld, J. & van Deventer, J., 1999. Effect of the Alkali Metal Activator on the Properties of Fly Ash-Based Geopolymers. 1 October, 38(10), pp. 3932-3941.

van Jaarsveld, J. & van Deventer, J., 1999. The effect of metal contaminants on the formation and properties of waste-based geopolymers. *Cement and Concrete Research,* August, 29(8), pp. 1189-1200.

van Jaarsveld, J., van Deventer, J. & Lukey, G., 2002. The effect of composition and temperature on the properties of fly ash- and kaolinite-based geopolymers. *Chemical Engineering Journal,* 28 October.89(1–3).

Verbeck, G., 1958. Carbonation of hydrated Portland cement. *Cement and Concrete,* pp. 17-36.

Wadsö, L., 2003. *An experimental comparison between isothermal calorimetry, semi adiabatic calorimetry and solution calorimetry for the study of cement hydration,* Finland: NORDTEST.

Wang, S.-D. & Scrivener, K. L., 1995. Hydration products of alkali activated slag cement. *Cement and Concrete Research,* April, 25(3), pp. 561-571.

Wang, S.-D., Scrivener, K. L. & Pratt, P., 1994. Factors affecting the strength of alkali-activated slag. *Cement and Concrete Research,* 24(6), pp. 1033-1043.

Xu, H. & Van Deventer, J., 2000. The geopolymerisation of alumino-silicate minerals. *International Journal of Mineral Processing,* June, 59(3), pp. 247-266.

Xu, H., van Deventer, J. S. J. & Lukey, G. C., 2001. Effect of Alkali Metals on the Preferential Geopolymerization of Stilbite/Kaolinite Mixtures. *Industrial & Engineering Chemistry Research,* 1 August, 40(17), pp. 3749-3756.

Yang, K. & Song, J., 2009. Workability Loss and Compressive Strength Development of Cementless Mortars Activated by Combination of Sodium Silicate and Sodium Hydroxide. *Journal of Materials in Civil Engineering,* 21(3), pp. 119-127.

Yang, K.-H., Song, J.-K., Ashour, A. F. & Lee, E.-T., 2008. Properties of cementless mortars activated by sodium silicate. *Construction and Building Materials,* September, 22(9), pp. 1981-1989.

Yip, C. & Lukey, G., 2005. The coexistence of geopolymeric gel and calcium silicate hydrate at the early stage of alkaline activation. *Cement and Concrete Research,* September, 35(9), pp. 1688-1697.

Zhao, F.-Q., Ni, W., Wang, H.-J. & Liu, H.-J., 2007. Activated fly ash/slag blended cement. *Resources, Conservation and Recycling,* 52(2), pp. 303-313.